

Surface Science

Room 104E - Session SS+AS+HC-MoM

Mechanistic Insights on Surface Reactions in Catalysis and at Novel Interfaces

Moderator: Bruce D. Kay, Pacific Northwest National Laboratory

8:20am **SS+AS+HC-MoM1 Study of Metal-Organic Complexation at Metal and Metal Oxide Surfaces** by HREELS, *Miao Wang, C. Williams, S.L. Tait*, Indiana University

The ordering of organic molecules at surfaces and the formation of ordered metal nanostructures at surfaces have been extensively studied for the advancement of organic photovoltaics, nanoscale molecular electronics, and catalysts. There are many chemical systems that benefit from the combination of organic ligands with single-site metal centers to design and tune specific chemistries, but metal-organic complexation at surfaces has not yet been significantly studied. Molecular ligands on a surface with specific binding pockets can bind metal centers to achieve uniform oxidation states, as has been shown in prior studies by our group and by other groups. The goal of these studies is to improve selectivity in heterogeneous catalysts and to develop other novel surface chemistries. With that end in mind, we present new experiments with metal-organic coordination on oxide support surfaces. Most of the metal-organic surfaces studies have been done on metal surfaces to facilitate surface analysis. We have studied the redox assembly of 3,6-Di-2-pyridyl-1,2,4,5-tetrazine (DPTZ) and Pt on oxide surfaces, including rutile $\text{TiO}_2(110)$ using High Resolution Electron Energy Loss Spectroscopy (HREELS), Auger Electron Spectroscopy (AES) and Low Energy Electron Diffraction (LEED). HREELS characterizes vibrational modes, which can provide key information about adsorbate interactions and metal-organic interactions at surfaces. DPTZ and Pt were sublimated onto the surface from a Knudsen-type evaporator. Submonolayer DPTZ vibrational modes were observed on $\text{Ag}(111)$ (C-H bending modes at 400 cm^{-1} , 618 cm^{-1} and 772 cm^{-1} ; ring deformation modes at 966 cm^{-1} , 1145 cm^{-1} and 1354 cm^{-1}) and on $\text{TiO}_2(110)$ (a ring deformation mode at 1580 cm^{-1} and a C-H stretching mode at 3060 cm^{-1}). To see the vibrational modes of adsorbates on TiO_2 , a Fourier deconvolution technique was applied to remove multiple excitations of surface phonon. Annealing DPTZ on $\text{Ag}(111)$ at 170°C caused significant changes to the HREEL spectra (C-H bending modes at 400 cm^{-1} and 740 cm^{-1} , ring deformation modes at 1100 cm^{-1} , 1445 cm^{-1} , 1574 cm^{-1} , a C-H stretching mode at 3080 cm^{-1}), but no observable changes were seen for DPTZ on $\text{TiO}_2(110)$ until the sample was annealed at 290°C . Adding equimolar Pt onto submonolayer DPTZ on $\text{Ag}(111)$ caused similar vibrational changes to be observed, but at a lower temperature of 140°C . HREELS studies of the Pt-DPTZ complex on $\text{TiO}_2(110)$, $\text{Au}(100)$, and other surfaces are ongoing. By studying the redox assembly of metal-organic complexes on these surfaces, strategies can be developed to customize and tune the reactivity of novel surface catalysts.

8:40am **SS+AS+HC-MoM2 Studies of Single-site Catalysts on Powdered Oxide Support through Redox Assembly**, *Linxiao Chen, J.P. McCann, S.L. Tait*, Indiana University

High levels of reaction selectivity for selective alkane functionalization are generally difficult to achieve with metal nanoparticle heterogeneous catalysts, due to the variety of metal binding sites available. Motivated by the desire towards the development of uniform single-site metal centers at surfaces, our group has been working on the redox assembly of metal-organic systems at surfaces. On a single crystal gold surface, electrons are transferred from platinum to the ligand 3,6-Di-2-pyridyl-1,2,4,5-tetrazine (DPTZ). Utilizing this unique redox chemistry, long-range ordered 1D chains with an alternating metal-ligand structure were assembled at deposition of DPTZ with pre-adsorbed metallic platinum. All platinum sites are oxidized into Pt(II) , and stabilized in the binding pocket between two DPTZ with identical chemical environment. Here, aiming at practical applications in catalysis, a novel solution-phase synthetic strategy was developed based on wet impregnation approach, in attempt to reproduce the similar metal-ligand structure on high-surface-area powdered oxide catalyst supports. X-ray photoelectron spectroscopy verified that the redox chemistry is applicable to real supports, and is crucial in the successful deposition of DPTZ despite a weak ligand-support interaction. The surface structure is further elucidated by X-ray diffraction and surface titration. It was concluded that the mobility of the metal and ligand on a rough support surface, and the existence of residual Cl from Pt precursors represent

major challenges. This metal-ligand structure can be manipulated by tuning strength of interaction between the supports, metal and ligand. Initial catalytic tests with the methane oxidation reaction exhibited C-H activation ability and selectivity similar to traditional highly-dispersed Pt catalysts. We have compared these catalysts and explored the limitations of single-site metal-organic complexes at oxide supports. Though being significantly stabilized by the favored coordination geometry and the redox chemistry, the thermal stability of the metal-ligand structure needs to be further enhanced.

9:00am **SS+AS+HC-MoM3 Controlled Reactions of Coordination Complexes on Oxide Surfaces**, *Susannah Scott*, University of California at Santa Barbara

INVITED

The reactions of coordination complexes with functional groups on oxide surfaces (acidic and basic hydroxyl groups, Lewis acidic cations and Lewis basic oxide anions) can lead to anchored metal complexes with a high degree of uniformity when conducted under carefully controlled conditions (low-to-moderate temperatures, absence of moisture and/or O_2). Detailed characterization of these sites using spectroscopic methods, elemental analysis and reactivity studies leads to information about their structure and insight into the underlying structure of the oxide surface. Experiments with gold and silver complexes such as $\text{Me}_2\text{Au}(\text{acac})$ and $\text{Ag}(\text{acac})$ reveal that interactions with surface hydroxyls involving strong H-bonding to ligand donor atoms are primarily responsible for their dispersion as isolated metal sites. By modulating the hydroxyl density via thermal pretreatment, it is possible to control not only the surface density of metal atoms, but also their subsequent mobility. In the case of nucleation and subsequent autocatalytic growth of metal nanoparticles, it is possible to exert control over particle size via the initial metal complex-oxide surface interaction.

9:40am **SS+AS+HC-MoM5 Adsorption and Activation of CO_2 on $\text{Cu}(997)$ at Low Temperature**, *Jun Yoshinobu*, The University of Tokyo, Japan

Adsorption and activation of carbon dioxide on $\text{Cu}(997)$ were investigated by infrared reflection absorption spectroscopy (IRAS), temperature programmed desorption (TPD), and X-ray photoelectron spectroscopy (XPS). CO_2 molecules are physisorbed on $\text{Cu}(997)$ at temperatures below 70 K . However, the vibrational spectra of adsorbed CO_2 depend significantly on the substrate temperature; IR spectra of CO_2 vibrational modes at 70 K show asymmetric Fano line shapes. On the other hand, at 85 K , the dissociation of CO_2 into CO was observed on $\text{Cu}(997)$ by IRAS and XPS, but not on $\text{Cu}(111)$. In addition, the reaction of CO_2 on $\text{Cu}(997)$ surface at 340 K under CO_2 gas pressure of 0.8 mbar was investigated by ambient pressure XPS. A main reaction product on the surface was identified as carbonate (CO_3), based on estimation of the composition ratio of oxygen to carbon. CO_3 was produced on the surface through the reaction of CO_2 with atomic oxygen formed from CO_2 dissociation.

10:00am **SS+AS+HC-MoM6 D_2O Interaction with Planar $\text{ZnO}(0001)$ Bilayer Supported on $\text{Au}(111)$: Structures, Energetics and Influence of Hydroxyls**, *Xingyi Deng, D.C. Sorescu, J. Lee*, National Energy Technology Laboratory

Ultrathin oxides with single or few atomic layers are considered new types of due to the emergence of film-specific structures with properties distinct from their bulk counterparts. $\text{ZnO}(0001)$ bilayer grown on $\text{Au}(111)$ adopts a planar, graphite-like structure via an intralayer relaxation from the bulk wurtzite structure. In this work, we investigate the interaction between D_2O and the planar $\text{ZnO}(0001)$ bilayer grown on $\text{Au}(111)$ with temperature programmed desorption (TPD), low energy electron diffraction (LEED), X-ray photoelectron spectroscopy (XPS), and density functional theory (DFT) calculations. D_2O molecules adsorbed on this planar surface form two ordered overlayers, a (3×3) and a $(\sqrt{3} \times \sqrt{3})R30^\circ$, not seen before on any of the bulk ZnO single crystal surfaces. The apparent activation energies of desorption (E_a) estimated from TPD peaks agree well with the adsorption energy values calculated from DFT. The DFT calculations also reveal that both overlayers are mediated by extensive hydrogen bonding among the molecules but with different packing densities. The hydroxyl groups, accumulating very slowly on the $\text{ZnO}(0001)$ bilayer surface under the standard ultrahigh vacuum (UHV) environment, strongly suppress the formation of the $(\sqrt{3} \times \sqrt{3})R30^\circ$ overlayer but have less impact on the (3×3) overlayer. We suggest that the difference in packing densities of the overlayers leads to these findings such that only the (3×3) overlayer with a more open structure can accommodate small amounts of the adsorbed hydroxyls.

Monday Morning, November 7, 2016

10:40am **SS+AS+HC-MoM8 Nanoscale Silicon as a Catalyst for Graphene Growth: Mechanistic Insight from In-Situ Raman Spectroscopy**, *Keith Share, R.E. Carter*, Vanderbilt University; *P. Nikolaev, D. Hooper*, Air Force Research Laboratory; *L. Oakes, A.P. Cohn*, Vanderbilt University; *R. Rao*, Air Force Research Laboratory; *A.A. Puretzky*, Oak Ridge National Lab; *D.B. Geohegan, B. Maruyama*, Air Force Research Laboratory; *C.L. Pint*, Vanderbilt University

Nanoscale carbons are typically synthesized by thermal decomposition of a hydrocarbon at the surface of a metal catalyst. Whereas the use of silicon as an alternative to metal catalyst could unlock new techniques to seamlessly couple carbon nanostructures and semiconductor materials, stable carbide formation in bulk silicon prevents the precipitation and growth of graphitic structures. Here, we provide evidence supported by comprehensive *in-situ* Raman experiments that indicates nanoscale grains of silicon in porous silicon (PSi) scaffolds act as catalysts for hydrocarbon decomposition and growth of few-layered graphene at temperatures as low as 700 K. Self-limiting growth kinetics of graphene with activation energies measured between 0.32 – 0.37 eV elucidates the formation of highly reactive surface-bound Si radicals that aid in the decomposition of hydrocarbons. Nucleation and growth of graphitic layers on PSi exhibits striking similarity to catalytic growth on nickel surfaces, involving temperature dependent surface and subsurface diffusion of carbon. This work elucidates how the nanoscale properties of silicon can be exploited to yield catalytic properties distinguished from bulk silicon, opening an important avenue to engineer catalytic interfaces combining the two most technologically-important materials for modern applications – silicon and nanoscale carbons.

11:00am **SS+AS+HC-MoM9 Functionalization of Graphene on Ru(0001) with Atomic Oxygen**, *Zbynek Novotny*, Pacific Northwest National Laboratory; *F.P. Netzer*, Karl-Franzens University, Austria; *Z. Dohnálek*, Pacific Northwest National Laboratory

Well-defined, monodispersed catalysts supported on oxidized carbon nanotubes are a promising class of new materials for heterogeneous catalysis. While such systems exhibit lower complexity compared to traditional catalysts, many questions, such as the reproducible preparation of carbon nanotubes and the range of functionalities used for anchoring of the clusters, make determination of their oxidation state and structure difficult. An analogous model system, graphene, can be prepared and studied under UHV conditions with great control. We employ scanning tunneling microscopy (STM) to study chemical functionalization of supported graphene on Ru(0001) with atomic oxygen. On Ru(0001) graphene forms a defect-free moiré structure with a periodicity of 3 nm, offering variety of distinct, regularly-spaced adsorption sites. Three different regions can be distinguished in STM images: bright regions (C atop of Ru) with the largest distance to the underlying Ru metal, dark hcp regions where graphene is closest to the metal, and medium-bright fcc regions where graphene is slightly further away compared to the hcp regions. Interestingly, for temperatures above 114 K, atomic oxygen (AO) is preferentially observed within the medium-bright fcc regions but in a minority of cases also in the hcp regions. The onset of AO mobility is observed at 400 K, where AO is occasionally moving inside the fcc region, or away from the less-stable hcp region towards the bordering fcc region. At higher temperatures (450-500 K), a dramatic increase in AO diffusion is observed allowing for AO transport between neighboring fcc regions through the hcp region. Upon encounter, the AO groups form stable immobile dimers and large clusters. The high-resolution time-lapsed data is used to assign the AO adsorption configuration to the on-top bonded enolate groups rather than the expected bridge-bonded epoxys. Our ongoing effort focuses on quantifying the enolate diffusion barrier and understanding their interactions with adsorbates such as H₂O, CO, and CO₂. The high thermal stability of enolate groups, and their large periodic separation (~3 nm) makes functionalized graphene/Ru(0001) an ideal model system for model studies of monodispersed catalysts.

11:20am **SS+AS+HC-MoM10 Interaction of BaO with H₂O, CO₂ and NO₂ Studied with APXPS and NEXAFS**, *Osman Karslioglu, I. Zegkinoglou, L. Trotochaud, H. Bluhm*, Lawrence Berkeley National Laboratory

Barium is a constituent of several technologically important materials such as NO_x storage and reduction (NSR) catalysts in automobiles, getters for UHV applications, perovskite catalysts for electrochemical reactions and high-temperature superconductors. Interaction of barium compounds with simple molecules such as H₂O, CO₂ and NO₂ is thus of practical importance. We studied the interaction of in-situ prepared BaO with H₂O, CO₂ and NO₂ as a function of temperature and pressure using ambient pressure X-ray photoelectron spectroscopy (APXPS) and near-edge X-ray absorption fine

structure (NEXAFS). Using in-situ preparation proved essential for preparing clean BaO, as the compound is extremely reactive even with minute amounts of H₂O and CO₂. We report the first experimental O K-edge X-ray absorption spectrum of clean BaO, for which the published spectra in the literature are more consistent with BaCO₃.

Surface Science

Room 104E - Session SS+AS+HC-MoA

Metals, Alloys, and Oxides: Reactivity and Catalysis

Moderator: David Mullins, Oak Ridge National Laboratory

1:40pm SS+AS+HC-MoA1 Scanning Tunneling Microscopy Studies of Hydrogen adsorption on the RuO₂(110) Surface, Arjun Dahal, R. Mu, Z. Dohnálek, I. Lyubinetzsky, Pacific Northwest National Laboratory

Understanding of hydrogen/oxygen interactions is important for a variety of fundamental and applied processes. By using high resolution scanning tunneling microscopy (STM), we probed the adsorption of H₂ (or D₂) on model catalyst RuO₂(110) surface, which has wide range of applications in heterogeneous catalysis, hydrogen storage, and many other energy related areas. Well-defined RuO₂(110) surface exposes alternating rows of bridge-bonded oxygen atoms (O_b) and five-fold-coordinated Ru atoms (Ru_{cus}). STM data indicate that hydrogen molecule dissociates even at 5 K, whereas one hydrogen adatom adsorbs on top of the Ru_{cus} site (producing a hydrate, H-Ru_{cus}, species) and the second on top of the adjacent O_b site (forming a bridging hydroxyl, H-O_b, species), generating an H-Ru_{cus}/H-O_b pair. For the low hydrogen coverage, the dissociated H-Ru_{cus}/H-O_b pairs adsorb on every alternate Ru_{cus}/O_b sites adopting a (2x1) registration. When RuO₂(110) surface adopts a such registration of the H-Ru_{cus}/H-O_b pairs locally, hydrogen starts to adsorb molecularly on top of the Ru_{cus} sites in between the adjacent dissociated hydrogen-pairs. With further increase of hydrogen coverage, linear arrays of H₂ molecules are formed along Ru_{cus} rows. The saturation coverage of the hydrogen on the RuO₂(110) surface is observed to be ~0.75 ML, where 1 ML is designated as the Ru_{cus} site density on the stoichiometric RuO₂(110) surface (5.06x10¹⁴ cm⁻²). Upon annealing the hydrogen-covered RuO₂(110) surface, H₂ molecules from the linear array desorb around 110 K. On the other hand, the H-Ru_{cus} species of H-Ru_{cus}/H-O_b pair transforms (via a proton transfer) into another H-O_b group, across-row from original H-O_b group, producing crosswise H-O_b/H-O_b pair at temperatures above ~250 K.

2:00pm SS+AS+HC-MoA2 Metal Vapor Adsorption Calorimetry on Layered Ca Niobate Nanosheets: Energetics and Adsorbate Structure, Wei Zhang, J. Lownsbury, University of Washington; R. Uppuluri, T.E. Mallouk, The Pennsylvania State University; C.T. Campbell, University of Washington

The metal/oxide interface is essential to many current and prospective technologies, including oxide-supported metal catalysts, fuel cells, photocatalysis, and nanoscale electronic contacts, so understanding the strength of metal – oxide bonding at such interfaces is of great interest. These strengths have been measured on single crystal oxide surfaces by single crystal adsorption calorimetry (SCAC) of metal atom adsorption in ultrahigh vacuum (UHV)¹ and on niobate and tantalate nanosheets by solution-based isothermal titration calorimetry during the deposition of transition metal oxide (or hydroxide) nanoparticles from their aqueous salt solutions^{2,3}. These niobate nanosheets are very interesting since they are highly ordered and essentially like single crystal surfaces in that the ratio of terrace sites to defect and edge sites is huge. Furthermore, when used as supports for transition metal oxide nanoparticles, they have been shown to display unusual stability against sintering.^{2,3} Here, we directly measure the adsorption energies of metal vapor on such niobate nanosheets using SCAC in UHV. Specifically, we study the adsorption of Ca and Ag vapor onto calcium niobate films that are 4 nanosheets thick (~4 nm total). Calcium atoms show a sticking probability near unity and an initial heat of adsorption of ~660 kJ/mol, much higher than the heat of bulk Ca(s) sublimation (178 kJ/mol). Low-energy ion scattering spectroscopy (LEIS), which is element-specific and probes only the topmost atomic layer, is used to investigate the resulting metal particle/film morphology. The possible chemical reactions between the metal vapor and the calcium niobate during adsorption are elucidated using X-ray photoelectron spectroscopy (XPS).

[1] Campbell, C. T.; Sellers, J. R. V. *Faraday Discussions* **2013**, 162, 9.

[2] Strayer, M. E.; Binz, J. M.; Tanase, M.; Shahri, S. M. K.; Sharma, R.; Rioux, R. M.; Mallouk, T. E. *J. Am. Chem. Soc.* **2014**, 136, 5687.

[3] Strayer, M. E.; Senftle, T. P.; Winterstein, J. P.; Vargas-Barbosa, N. M.; Sharma, R.; Rioux, R. M.; Janik, M. J.; Mallouk, T. E. *J. Am. Chem. Soc.* **2015**, 137, 16216.

2:20pm SS+AS+HC-MoA3 Structure and Reactivity of Model Iron Oxide Surfaces, Gareth Parkinson, TU Wien, Austria

INVITED

Iron oxides are abundant in nature and extensively utilized in modern technologies including heterogeneous catalysis [1]. Magnetite (Fe₃O₄), for example, is the active phase of the industrial water-gas shift catalyst, while hematite (Fe₂O₃) is used as the photoanode for photoelectrochemical water splitting. In this talk I will discuss our recent investigations of the Fe₃O₄(100) and Fe₂O₃(1-102) surfaces using a combined experiment/theory approach. The Fe₃O₄(100) surface forms a reconstruction based on an ordered array of subsurface cation vacancies that contains exclusively Fe³⁺, and is relatively inert [2]. Although formic acid adsorbs dissociatively at regular lattice sites [3], methanol adsorption is restricted to defects containing Fe²⁺ [4]. The bulk of the talk will focus on a detailed study of water adsorption on Fe₃O₄(100) by TPD, STM, XPS, UPS, DFT+U and molecular dynamics calculations. In the remaining time I will demonstrate that a bulk terminated Fe₂O₃(1-102) surface can be prepared by annealing in 10⁻⁶ mbar O₂, and a reduced (2x1) surface forms rapidly when heating in UHV. The structure of the (2x1) reconstruction and its reactivity toward water will be discussed.

[1] G.S. Parkinson, Iron oxide surfaces, *Surface Science Reports* (2016), <http://dx.doi.org/10.1016/j.surfrep.2016.02.001>

[2] R. Bliem, E. McDermott, P. Ferstl, M. Setvin, O. Gamba, J. Pavelec, M.A. Schneider, M. Schmid, U. Diebold, P. Blaha, L. Hammer, G.S. Parkinson, *Subsurface Cation Vacancy Stabilization of the Magnetite (001) Surface*, *Science* **346** (2014) 1215-1218.

[3] O. Gamba, H. Noei, J. Pavelec, R. Bliem, M. Schmid, U. Diebold, A. Stierle, G.S. Parkinson, Adsorption of Formic Acid on the Fe₃O₄(001) Surface, *The Journal of Physical Chemistry C* **119** (2015) 20459-20465.

[4] O. Gamba, J. Hulva, J. Pavelec, R. Bliem, M. Schmid, U. Diebold, G.S. Parkinson, The role of surface defects in the adsorption of methanol on Fe₃O₄(001), *Topics in Catalysis* submitted (2016).

3:00pm SS+AS+HC-MoA5 Structure and Ethanol Reactivity of Ti-modified CeO₂(111) Mixed Oxide Surfaces, E.W. Peterson, Jing Zhou, University of Wyoming

Ceria has been widely studied as an oxidation-reduction catalyst due to its unique redox properties and oxygen storage capacity. There has been an interest to incorporate additional metal dopants such as Ti into ceria to potentially enhance the thermal stability as well as improve the redox properties for practical applications in catalysis. This paper focuses on the fundamental mechanistic understanding of the effect of Ti dopant on the structure and reactivity of ceria using scanning tunneling microscopy, X-ray photoelectron spectroscopy, infrared spectroscopy and temperature programmed desorption techniques. In the study, submonolayer coverage of Ti was deposited on well-ordered CeO₂(111) (1.5<x<2) thin films at room temperature. XPS studies show that Ti is oxidized to Ti⁴⁺ at the cost of Ce⁴⁺ reduction. Observation of CO IR band at 2173 cm⁻¹ further confirms the presence of titania on the ceria surface. At 300 K, small atomic-like features of Ti-O-Ce linkages are present on ceria, which can coalesce into chain structures after heating to 700 K. Upon ethanol adsorption at 300 K, ethoxy was the surface intermediate observed on both oxidized and partially reduced ceria surface. With heating, it can go through the dehydration or dehydrogenation process to form acetaldehyde, ethylene, water and hydrogen products. Our studies have demonstrated that addition of Ti in ceria can affect the dehydration and dehydrogenation selectivity. Furthermore, the nature of ceria supports associated with oxygen vacancies and Ti dopants can have a promotional effect in the stability of deposited metal nanoparticles, such as Ni, and the chemical behavior toward the adsorption and reaction of ethanol. The research is sponsored by the National Science Foundation Career Grant (Award Number: CHE1151846) and the Wyoming NASA EPSCoR (NASA Grant: NNX13AB13A).

3:20pm SS+AS+HC-MoA6 New Insights into the Coverage-Dependent Structure and Desorption Kinetics of CO on Palladium(111), Pan Xu, Stony Brook University; S.-Y. Hong, Brookhaven National Laboratory; S. Liu, Stony Brook University; N.R. Camillone, M.G. White, N. Camillone, Brookhaven National Laboratory

Carbon monoxide adlayers on palladium surfaces have, since the early days of ultrahigh-vacuum surface science, served as model systems for the study of molecule-surface interactions, structure and dynamics. As part of a recent study of the dynamics of ultrafast molecule-surface energy transfer we have revisited the CO/Pd(111) system and found that it continues to teach us about the complexities of molecule-surface interactions. Specifically, it has long been known that CO adlayers assume a wide range

of ordered structures on Pd(111) at low temperature (~80 K). In fact, between the ($\sqrt{3}\times\sqrt{3}$)R30° 0.33-ML and (2×2) 0.75-ML (saturation) structures, at least 17 well-ordered structures have been identified. Until now, however, a comprehensive correlation between these structures and the thermal desorption kinetics has not been reported. In this talk we detail a systematic investigation that correlates individual temperature-programmed desorption (TPD) features with specific adlayer structural phase transitions. We report that in addition to the spectrum of previously-observed structures we have observed for the first time, to the best of our knowledge, a well-developed, ordered domain-boundary structure at a coverage just below saturation. We have assigned this structure as a c(16×2) adlayer comprised of stripes with local (2×2) structure and used density functional theory to investigate the adsorption site preferences within the adlayer. We show how our results, in combination with existing data, can be interpreted in terms of a compromise between the energy minimization that accompanies binding at high-symmetry sites and lateral repulsive interactions. Furthermore, we describe how quantifying the coverage using the integrated desorption yield areas is problematic due to difficulties in growing a fully-saturated adlayer. We attribute these difficulties to a kinetic limitation of the structural phase transitions at high coverage, and show that this limitation is easily addressed by preparing the adlayer at a somewhat elevated temperature. We also detail use of the inversion-optimization method to extract the coverage dependence of the desorption activation energy from the TPD measurements. We compare the resultant simulated TPD line shapes with those derived using the "leading-edge" analysis method.

4:00pm SS+AS+HC-MoA8 Combined Experimental and Computational Study of Water on Fe₃O₄ (001), Jan Hulva, Vienna University of Technology, Austria; **M. Meier,** Universität Wien, Austria; **J. Pavelec, S. Maaß, R. Bliem, M. Schmid, U. Diebold,** Vienna University of Technology, Austria; **C. Franchini,** Universität Wien, Austria; **G.S. Parkinson,** Vienna University of Technology, Austria

The interaction of water with metal-oxide surfaces is an important topic for a wide range of technological and environmental applications. This is particularly true for the iron oxides because of their abundance in nature and their use in chemical processes where water is involved e.g. the water-gas shift reaction [1]. Recent studies of water on iron oxide surfaces have found significant complexity, with evidence for pressure dependent adsorption, mixed-mode adsorption and coverage dependent hydrogen bonding [2-4]. Here we use a multi-technique experimental approach combined with ab-initio calculations including molecular dynamics to disentangle the coverage and temperature dependent behavior of water on the reconstructed Fe₃O₄(001)-(√2x√2)R45° surface [5].

Temperature programmed desorption shows that the first monolayer of water desorbs from the surface in four distinct peaks between 150 K and 250 K. Based on XPS, STM images and ab-initio calculations, we conclude that the first three peaks originate from molecular water desorbing from a coverage-dependent hydrogen-bonded network, while the last peak results from recombinative desorption from a partially dissociated water trimer species. Two additional desorption states at 340 K and 520 K are ascribed to desorption from surface defects and recombinative desorption of the surface surface hydroxyl groups, respectively.

- [1] Parkinson, G.S., "Iron oxide surfaces", *Surface Science Reports* (2016)
- [2] Dementyev, P., et al. "Water Interaction with Iron Oxides." *Angew.Chem. Int. Ed.* 54 (2015): 13942
- [3] Mulakaluri, N., et al. "Partial dissociation of water on Fe₃O₄ (001): Adsorbate induced charge and orbital order." *Phys. Rev. Lett.* 103 (2009): 176102.
- [4] Kendelewicz, T., et al. "X-ray photoemission and density functional theory study of the interaction of water vapor with the Fe₃O₄ (001) surface at near-ambient conditions." *J. Phys. ChemC* 117 (2013): 2719-2733.
- [5] Bliem, R., et al. "Subsurface cation vacancy stabilization of the magnetite (001) surface." *Science* 346 (2014): 1215-1218.

4:20pm SS+AS+HC-MoA9 Water Desorption from Sulfur-Doped Oxide Thin Films on W (100), Anthony Babore, J.C. Hemminger, University of California Irvine

Recent first principle calculations by Pacchioni and coworkers¹ suggest that sulfur dopants incorporated into the WO₃ lattice could favorably shift the band gap for enhanced visible light absorption. The present study aims to gain fundamental insight into the reactivity of a simple sulfur doped tungsten oxide system by using temperature programmed desorption (TPD) and water (D₂O) as a probe molecule. Furthermore, water desorption

spectra were also obtained for pure oxide and pure sulfide films on W (100) for comparison. Auger electron spectroscopy (AES) was used to confirm the presence and relative amounts of sulfur and oxygen on the surface. TPD was then used to monitor the m/z 20, 19, and 18 signal intensity as a function of the temperature. To quantify the reactivity of water on the surface, activation energies of desorption were obtained. The results indicate distinct differences in the desorption spectra and desorption energies that exemplify the reactivity of each of the surfaces.

1. Wang F, Di Valentin C, Pacchioni G (2012) *J Phys Chem C* 116:8901–8909

4:40pm SS+AS+HC-MoA10 Adsorption and Decomposition of Dimethyl Methylphosphonate on Metal Oxide Surfaces Under Atmospheric Conditions, Ashley Head, L. Trotochaud, Lawrence Berkeley National Laboratory (LBNL); **R. Tsyshevsky,** University of Maryland College Park; **O. Karslioglu,** Lawrence Berkeley National Laboratory (LBNL); **M.M. Kukulja,** University of Maryland College Park; **H. Blum,** Lawrence Berkeley National Laboratory (LBNL)

Organophosphonates are used as corrosion inhibitors, pesticides, insecticides, and chemical warfare agents. This class of molecules has a range of acute toxicity, so dimethyl methylphosphonate is commonly used as a proxy for more toxic molecules. Metal oxides are used in applications for binding and decomposing organophosphonates despite little understanding of the chemistry and reactivity, especially in the presence of atmospheric molecules. With the ability to collect photoemission spectra at pressures up to about 25 Torr, ambient pressure XPS is well-suited to investigate the adsorption of DMMP in the presence of other molecules that have relevance to applications. Using MoO_x and CuO_x foils as model systems for chemical filtration materials, we have studied the adsorption and decomposition behavior of DMMP and how this behavior changes in the presence of atmospherically relevant molecules, including water, hydrocarbons, and NO_x. The effect of the small molecules on the substrate and the subsequent effects on DMMP binding, coverage, and decomposition will be discussed. APXPS results are interpreted with the aid of density functional theory calculations, which model DMMP adsorption, decomposition products, and reaction energies.

5:00pm SS+AS+HC-MoA11 Oxygen Chemisorption and Thermal Oxidation of TiAlN High Power Pulsed Magnetron Sputtering Hard Coatings, Martin Wiesing, T. de los Arcos, G. Grundmeier, University of Paderborn, Germany

The thermal oxidation of Ti_{0.5}Al_{0.5}N hard coatings as deposited by High Power Pulsed Magnetron Sputtering was investigated at reduced oxygen partial pressures of 10⁻⁶ and 10⁻² Pa in a temperature range from 298 to 800 K. Quasi in-situ X-ray Photoelectron Spectroscopy and Low Energy Ion Scattering studies revealed oxygen to bind selectively to Ti-sites on the surface [1] and oxygen migration into the near-surface region. Three dimensional oxidation leads to the formation of a double layered surface oxide including a TiAl(O,N) growth region [2] terminated with a Ti^{IV} containing surface oxide [3]. Based on Wagner plot analysis, the surface oxide layer formed at 800 K can be described by a mixed Ti^{IV}Al^{III}O_x phase while a separated (Ti^{IV}O₂)(Al^{III}₂O₃) phase preferentially forms at 298 K. Complementary Ultraviolet Photoelectron Spectroscopy revealed a high degree of nitrogen doping in both cases.

The results are of importance for the design of multi-layered nitridic hard coatings and for a thorough understanding of the high-temperature oxidation resistance of such coatings.

Acknowledgement: The authors gratefully acknowledge the German Research Foundation (DFG) for financial support (SFB–TR 87). We thank Prof. Dr. J. Schneider and Holger Rueß for providing the coated specimen.

References:

- [1] C. Kunze, D. Music, M. to Baben, J.M. Schneider, G. Grundmeier, Temporal evolution of oxygen chemisorption on TiAlN, *Appl. Surf. Sci.* 290 (2014) 504–508. doi:10.1016/j.apsusc.2013.11.091.
- [2] S. Hofmann, Formation and diffusion properties of oxide films on metals and on nitride coatings studied with Auger electron spectroscopy and X-ray photoelectron spectroscopy, *Thin Solid Films.* 193–194, Part 2 (1990) 648–664. doi:10.1016/0040-6090(90)90216-Z.
- [3] C. Gnath, C. Kunze, M. Hans, M. to Baben, J. Emmerlich, J.M. Schneider, G. Grundmeier, Surface chemistry of TiAlN and TiAlNO coatings deposited by means of high power pulsed magnetron sputtering, *J. Phys. Appl. Phys.* 46 (2013) 084003. doi:10.1088/0022-3727/46/8/084003.

Surface Science

Room 104D - Session SS1+AS+HC+NS-TuM

Surface Dynamics, Non-Adiabaticity, and Theory and Modeling of Surface and Interfacial Phenomena

Moderator: Greg Kimmel, Pacific Northwest National Laboratory

8:00am **SS1+AS+HC+NS-TuM1 Graphene-Semiconductor Catalytic Nanodiodes for Quantitative Detection of Hot Electrons Induced by a Chemical Reaction**, *Hyosun Lee**, KAIST & IBS, Republic of Korea; *I. Nedrygailov*, IBS & KAIST, Republic of Korea; *Y.K. Lee, C. Lee*, KAIST & IBS, Republic of Korea; *H. Choi*, Electronics and Telecommunications Research Institute (ETRI), Republic of Korea; *J.Y. Park*, Institute for Basic Science (IBS) & Korea Advanced Institute of Science and Technology (KAIST), Republic of Korea

Direct detection of hot electrons produced by exothermic reactions on catalysts is an effective strategy to quantify the non-adiabatic energy transfer during the elementary steps of the surface reactions, which provides an insight of the catalytic activity.^{1,2} In particular, hot electron dynamics at the surface of metal nanoparticles (NPs) with precisely controlled shape and size is a challenge as well as a key issue in the real-world catalyst system. Herein, we show a novel scheme of graphene catalytic nanodiode composed of a Pt NPs array on graphene/TiO₂ Schottky nanodiode, which allows detection of hot electron flows induced by hydrogen oxidation on Pt NPs. By analyzing the correlation between the turnover rate (catalytic activity) and hot electron current (chemicurrent) measured on the graphene catalytic nanodiodes, we demonstrate that the catalytic nanodiodes utilizing a single graphene layer for electrical connection of Pt NPs are beneficial for the detection of hot electrons due to not only atomically thin nature of graphene but also reducing the height of the potential barrier existing at the Pt NPs/graphene interface. Thereby, the graphene catalytic nanodiodes offer an effective and easy to use approach to study mechanisms of chemical energy conversion in various heterogeneous system, even including composite catalysts with carbon-based supports.

References

1. H. Lee, I. I. Nedrygailov, Y. K. Lee, C. Lee, H. Choi, J. S. Choi, C. Choi, J. Y. Park, *Nano Lett.* 16 (2016) 1650-1656.
2. H. Lee, I. I. Nedrygailov, C. Lee, G. A. Somorjai, J. Y. Park, *Angew. Chem. Int. Ed.* 54 (2015) 2340-2344.

8:20am **SS1+AS+HC+NS-TuM2 Adlayer-Structure Dependent Ultrafast Desorption Dynamics: The Coverage Dependence of Substrate-Adsorbate Energy Transfer in Carbon Monoxide on Pd(111)**, *Sung-Young Hong*, Brookhaven National Laboratory; *P. Xu*, Stony Brook University; *N.R. Camillone, M.G. White, N. Camillone*, Brookhaven National Laboratory

We have conducted a detailed investigation of the coverage dependence of the ultrafast photoinduced desorption of CO from the (111) surface of palladium. Because the CO binding site depends on coverage, these measurements present an opportunity to examine the dependence of the substrate-adsorbate energy transfer on adsorption site. Specifically, as the CO coverage is increased, the adsorption site population shifts from all three-fold hollow (up to 0.33 ML), to bridge and near bridge (> 0.5–0.6 ML) and finally to mixed three-fold hollow plus top site (0.6 ML to saturation at 0.75 ML). We show that between 0.24 and 0.75 ML this progression of binding site motifs is accompanied by two remarkable features in the ultrafast photoinduced desorption of the adsorbates: (i) a roughly two-orders of magnitude increase in the desorption probability, and (ii) a nonmonotonic variation in the adsorbate-substrate energy transfer rate observed in two-pulse correlation experiments, with a minimum occurring at intermediate coverages. Simulations using a phenomenological model to describe the adsorbate-substrate energy transfer in terms of frictional coupling indicate that these features are consistent with an adsorption-site dependent electron-mediated energy coupling strength, η_{el} , that decreases with binding site in the order: three-fold hollow > bridge and near bridge > top site. The weakening of η_{el} largely counterbalances the decrease in the desorption activation energy that accompanies this progression of adsorption site motifs and moderates what would otherwise be a rise of several orders of magnitude in the desorption probability. Furthermore, we show that within this framework, the observed energy transfer rate enhancement at saturation coverage is due to interadsorbate energy

transfer from the copopulation of molecules bound in three-fold hollows to their top-site neighbors. This conclusion is supported by comparison to desorption of CO from mixed CO+O adlayers where the O adsorbs at three-fold hollow sites and further promotes CO desorption from top sites.

8:40am **SS1+AS+HC+NS-TuM3 Evidence for a Spin Accelerated Reaction Mechanism in the Thermal Decomposition of Alkyl Radicals on the Si(100) Surface**, *A.J. Pohlman, D.S. Kaliakin, S.A. Varganov, Sean Casey*, University of Nevada

Density functional theory and complete active space self-consistent field calculations were used to probe the thermal decomposition of alkyl radicals on the Si(100) surface. Single dimer and single row double dimer cluster models were used to mimic the Si(100) surface in the calculations, and results indicate an interdimer β -hydrogen elimination reaction is the kinetically favored thermal decomposition pathway for adsorbed alkyl radicals. This pathway occurs via a spin crossing from the initial singlet energy surface to the triplet surface mediated by spin-orbit coupling. On the triplet surface the barrier to the elimination reaction is predicted to be about 40 kJ/mol lower than on the singlet surface. Experimental thermal desorption studies of alkyl chlorides adsorbed onto the Si(100)-(2x1) surface appear to give desorption energies for alkene products that are consistent with the barriers computed for the interdimer β -hydrogen elimination spin accelerated reaction mechanism. Experimental and computational results for the adsorption/desorption energetics of several different alkyl radicals will be discussed, along with results from partial deuteration studies of adsorption of selected haloalkanes.

9:00am **SS1+AS+HC+NS-TuM4 Hyperthermal Ion Induced Hot Carrier Excitations in a Metal Probed using Schottky Diodes**, *Dhruba Kulkarni, D.A. Field, D.B. Cutshall, J.E. Harriss, W.R. Harrell, C.E. Sosolik*, Clemson University

We present measurements on hot carrier excitations in a metal irradiated by hyperthermal energy ions.

Specifically, alkali (Na⁺/Rb⁺) and noble gas (Ar^{q+}) ions were used to irradiate a Schottky diode consisting of

a thin film of Ag (~25nm) grown on an n-type Si (111) wafer. Measurements of the resultant current

through the device were performed as a function of energy, angle of incidence and velocity of the

incident ions. Energy loss of the incident energetic ions inside the metal film leads to the generation of

hot carriers that travel ballistically to the Schottky interface and are detected as a kinetically-induced

current or “kinecurrent” within the device. This kinecurrent is analogous to previous measurements of

“chemicurrent” [H. Nienhaus, *Surface Science*, **45**, 1-78 (2002)], which were linked to the energy

delivered to a surface by exothermic reactions that could non-adiabatically couple to the electronic

structure and generate hot carriers.

9:20am **SS1+AS+HC+NS-TuM5 H Atom Scattering, Adsorption, and Absorption in Collisions with Metal Surfaces: the crucial role of electron-hole-pair excitation**, *M. Alducin*, Donostia International Physics Center, Spain; *Daniel Auerbach*, Max Planck Institute for Biophysical Chemistry, Germany; *M. Blanco-Rey*, Donostia International Physics Center, Spain; *O. Bünermann, Y. Dorenkamp*, Georg-August University of Göttingen; *S.M. Janke*, Max Planck Institute for Biophysical Chemistry, Germany; *H. Jiang*, Georg-August University of Göttingen; *A. Kandratenka*, Max Planck Institute for Biophysical Chemistry; *G.-J. Kroes*, Leiden Institute of Chemistry, The Netherlands; *M. Kammler*, Max Planck Institute for Biophysical Chemistry; *M. Pavenlo*, Leiden Institute of Chemistry **INVITED**

When an H atom collides with a solid surface, it can transfer some of its kinetic energy into elementary excitations of the solid like phonons and electron-hole pairs. If the atom loses enough kinetic energy, it can become bound to the solid, either on the surface or in the bulk. For a metal, the availability of a continuum of low lying electronic excitations can lead to the breakdown of the adiabatic Born Oppenheimer approximation and the facile nonadiabatic excitation of electron-hole pairs (ehp). If the H atom loses sufficient energy, it can enter a bound state with the solid, either on the surface or in the bulk.

We have used a combined theoretical and experimental approach to elucidate the relative roles of adiabatic processes (phonon excitation) and

* National Student Award Finalist

Tuesday Morning, November 8, 2016

nonadiabatic processes (ehp excitation) in collisions of H atoms with metals, insulators, and graphene. The experiments use photolysis to produce nearly mono-energetic beams of H atoms with energies of 1 - 3.3 eV and high resolution energy loss measurements using Rydberg atom tagging time-of-flight analysis. The theory involves calculations of classical trajectories for H atom collisions with two techniques. In the first, we calculate energies and forces on-the-fly during the course of a trajectory using density functional theory (DFT) and ab initio molecular dynamics (AIMD). In the second, we construct a full dimensional potential energy surface (PES) using a flexible functional form fit to DFT energies and bulk properties of the solid.

The measured mean energy loss for H atoms scattering from metals is large, approximately 30% of the initial energy and there is a tail in the energy loss distribution (ELD) extending to the full energy of incidence. The measured ELD is in reasonable agreement with theory only if nonadiabatic effects are included; adiabatic theory drastically underestimates the energy loss. Scattering from insulators (where ehp excitation can be excluded) shows much smaller energy loss and results consistent with adiabatic theory.

For metals, nonadiabatic effects not only dominate the energy loss process, but also change both the magnitude and mechanism for adsorption on metals. With nonadiabatic effects, the most probable pathway to adsorption is for H atoms to penetrate the surface, lose energy in the subsurface region, and then reemerge to adsorb on the surface.

11:00am SS1+AS+HC+NS-TuM10 Progress in Characterizing Submonolayer Island Growth: Capture-Zone Distributions, Growth Exponents, and Transient Mobility, Theodore L. Einstein, University of Maryland, College Park; A. Pimpinelli, Rice University; J.R. Morales-Cifuentes, University of Maryland, College Park; D.L. González, Universidad del Valle, Colombia
Analyzing capture-zone distributions (CZD) using the generalized Wigner distribution (GWD) has proved a powerful way to gain insight into epitaxial growth, in particular to access the critical nucleus size i , as reviewed in [1]. The CZ of an island contains all points closer to that island than to any other and is known as a Voronoi tessellation. This approach complements measurements of the growth exponent α from the scaling (with flux F) of island density $N \sim F^\alpha$ and of the distribution of island sizes. We summarize some extensive Monte Carlo simulations and experiments, especially newer ones, on various systems to which the GWD has been applied. These experiments include atomic or organic adsorbates, sometimes with impurities, and colloidal nano-particles. In some cases, most notably parahexaphenyl (6P) on sputter-modified mica [2], the value i extracted from CZD differs from the [larger] values of i deduced from $N \sim F^\alpha$. Furthermore, while the scaling was good, the values of α differed considerably at small and large F , which was attributed to DLA and ALA dynamics [2]. To reconcile the CZD and scaling measurements, we took into account long-known transient mobility (hot precursors) using a rate-equation approach [3]. We also applied this method to data for pentacene (5A) on the same substrate. In applications of the GWD to social phenomena, notably the areas of secondary administrative units (e.g. counties or French *arrondissements*) [4], lognormal distributions (typically due to multiplicative noise) sometimes arise instead of GWD or gamma distributions; we show this also occurs for some pore-size distributions [5].

*Work at UMD supported by NSF CHE 13-05892

[1] T.L. Einstein, A. Pimpinelli, D.L. González, J. Cryst. Growth **401** (2014) 627; TLE, AP, DLG, J.R. Morales-Cifuentes, J. Physics: Conf. Ser. J. Phys.: Conf. Series **640** (2015) 012024

[2] T. Potocar et al., Phys. Rev. B **83** (2011) 075423 & later work by A. Winkler et al., see [1].

[3] JRM-C, TLE, and AP, Phys. Rev. Lett. **113** (2014) 246101.

[4] R. Sathiyarayanan, Ph.D. thesis, UMD, 2009; R. Sathiyarayanan and TLE, preprint.

[5] A.S. DeLoach, B.R. Conrad, TLE, and D.B. Dougherty, submitted.

11:20am SS1+AS+HC+NS-TuM11 Hindered Translator and Hindered Rotor Models for Calculating the Entropy of Adsorbed Species, Lynza H. Sprowl, Oregon State University; C.T. Campbell, University of Washington; L. Arnadottir, Oregon State University

Adsorbed species on surfaces are important for a range of applications including heterogeneous catalysis, corrosion processes, and film growth. The need for a fast and accurate way to predict equilibrium constants and

rate constants for surface reactions is important for understanding reaction kinetics and for building microkinetic models of catalytic reactions. Here a method to calculate partition functions and entropy of adsorbed species is presented. Instead of using the vibrational frequencies estimated from density functional theory and the harmonic oscillator approximation to calculate the partition function for all modes of motion, we use hindered translator and hindered rotor models for the three modes of motion parallel to the surface, two translations and one rotation. The energy barriers for translation and rotation were determined using density functional theory and the nudged elastic band method for four different adsorbates on a platinum surface: methanol, propane, ethane, and methane. The hindered translator model was used to calculate the entropy contributions from the two translations parallel to the surface and the hindered rotor model was used to calculate the entropy contribution from the rotation about the axis perpendicular to the surface. When combined with the vibrational entropy contributions and the concentration related entropy contributions, this gives the total entropy of the adsorbate on the surface. The total adsorbate entropies were found to agree well with experimental results, with an average absolute value of the error of only 1.1R or 8% for the four adsorbates. This new model should be useful to future researchers in surface chemistry, since it provides more accurate predictions of standard-state entropies and partition functions, and thus more accurate equilibrium constants and rate constants for surface reactions than provided by the standard harmonic oscillator approximation.

11:40am SS1+AS+HC+NS-TuM12 Stabilization of X-Au-X Complexes on the Au(111) Surface: A Theoretical Investigation and Comparison of X=Sulfur, Chlorine, Methylthiolate, and Silylthiolate, J. Lee, J.S. Boschen, T.L. Windus, P.A. Thiel, J.W. Evans, Da-Jiang Liu, Iowa State University

The involvement of Au atoms in the self-assembled methylthiolate (CH_3S) monolayers on Au(111) has been demonstrated experimentally [1], while for S and Cl, chain-like structures with no direct Au involvement were found [2,3]. We find that for S on various coinage metal surfaces, the linear S-M-S complexes (M=Cu, Ag, Au) are prevalent. A systematical theoretical study of the X-Au-X complexes, with X=S, Cl, CH_3S , and SiH_3S , has been performed using DFT and other quantum chemistry methods. Assuming equilibration of the metal substrate, the chemical potential of X are calculated and used to predict the stability of various Au-X complexes. We find good agreement between DFT and available experimental findings. Furthermore, the van der Waals interaction is shown to play a crucial role in the self-assembly of CH_3S observed in experiments [1].

[1] P. Maksymovych, O. Voznyy, D. B. Dougherty, D. C. Sorescu, J. T. Yates Jr., *Prog. Surf. Sci.* **85**, 206 (2010).

[2] V. V. Zheltov et al. *Phys. Rev. B*, **89**, 195425 (2014).

[3] H. Walen, *J. Chem. Phys.* **143**, 014704 (2015).

12:00pm SS1+AS+HC+NS-TuM13 Contrasting Phonon Confinement and Interface Stability at Fe-Ag and Fe-Cr Multilayers: Insights from Ab Initio Calculations, S. Hong, Talat Rahman, University of Central Florida

We have performed density functional theory based calculations to compare the characteristics of the interface of Fe-Ag and Fe-Cr multilayers. A perfect interface lattice match between the Fe and Ag layers was obtained by rotating fcc Ag(100) layers by 45° on bcc Fe(100). On the other hand, the Fe-Cr interface could be modeled by epitaxial layers of bcc Fe(100) and Cr(100). In Fe-Ag multilayers, we find the signature peak of Fe bulk phonons (35 meV) to be completely diminished, while the low energy peaks are remarkably enhanced, in agreement with experiment [1]. In contrast, the phonon density of state in the Fe-Cr multilayers do not show any salient feature except a slight decrease in the 35 meV peak for the Fe layer at the interface, as compared to that of the middle Fe layer, again in agreement with experiment [2]. The magnetic moment of the interfacial Fe atoms is larger than that of Fe atoms in other layers, as a result of charge transfer from Fe to Ag at the interface. As compared to the middle layers, more spin-up and less spin-down states are occupied at the interface in such a way that Fe donates a large number of spin-down electrons to Ag but receives only a few spin-up electrons from the latter because of the almost fully occupied Ag d-band. This leads to rather unstable Fe-Ag interface. On the contrary, at the Fe-Cr interface, Cr can easily give and take electrons leading to smooth interfacial coupling and stable environment.

[1] B. Roldan Cuenya et al., to be published

[2] Roldan et al, *Phys. Rev. B* **77**, 165410 (2008).

Work supported in part by DOE Grant No. DOE-DE-FG02-07ER46354

Surface Science

Room 104E - Session SS2+AS+HC+NS-TuM

Nanostructures: Growth, Reactivity, and Catalysis

Moderator: Bruce Koel, Princeton University

8:00am **SS2+AS+HC+NS-TuM1 Use of Size Correlations to Probe Reaction Mechanisms on Size-selected Model Catalysts**, *Scott Anderson*, University of Utah **INVITED**

The ability to prepare model catalysts by deposition of mass-selected metal clusters allows the size and density of catalytic sites to be varied independently and precisely, providing a new tool for mechanistic studies. In addition, preparation of truly monodisperse samples alters the kinetics for Ostwald ripening, thus changing the cluster stability under thermal/reactive conditions. This talk will focus on use of size-dependent correlations between catalytic activity and physical properties such as cluster morphology and electronic properties, to probe the factors that control catalysis and electrocatalysis by supported Pt clusters in the <25 atom size range. The stability of the clusters, and how this varies with size under heating, adsorbate exposure, and potential cycling will also be discussed.

8:40am **SS2+AS+HC+NS-TuM3 Role of the Strong Metal Support Interaction on the Catalytic Activity of Platinum Deposited on TiO₂ Supports**, *R.Paul Hansen, R.S. Phillips*, University at Albany-SUNY; *E.T. Eisenbraun, C.A. Ventrice, Jr.*, SUNY Polytechnic Institute

Several roadblocks prevent the large-scale commercialization of hydrogen fuel cells, including the stability of catalysts and their substrates and the high cost of the Pt involved in the oxygen reduction reaction (ORR). The former of these problems can be solved by replacing the traditional carbon support with a conductive metal oxide such as reduced TiO₂, which will not easily corrode and should result in longer lasting fuel cells. The Pt is necessary in the cathode of the fuel cell to overcome the slow kinetics of the ORR. In this study, Pt was deposited either by atomic layer deposition (ALD) or physical vapor deposition (PVD). The typical size of the Pt islands that were grown using these deposition techniques was 5-8 nm. One factor that can inhibit the catalytic activity of a metal catalyst on a metal oxide is the strong metal support interaction (SMSI). This is where a metal on a reducible metal oxide can be encapsulated by a layer of the metal oxide support material at elevated temperatures. The processing of materials through atomic layer deposition can exceed this temperature. The TiO₂ substrates used in this study were either grown by ALD, which results in a polycrystalline anatase film, or were single-crystal rutile TiO₂(110) samples prepared in ultra-high vacuum (UHV). The Pt/TiO₂ samples were tested electrochemically using cyclic voltammetry (CV) to determine the level of catalytic activity. To determine the effect of the SMSI interaction on the catalytic activity of the PVD grown samples, CV was performed on samples that were annealed in high vacuum after Pt deposition. Additional characterization was performed with scanning electron microscopy (SEM), Auger electron spectroscopy (AES), x-ray photoelectron spectroscopy (XPS), Rutherford backscattering spectrometry (RBS), and four point probe analysis.

9:00am **SS2+AS+HC+NS-TuM4 Adsorption and Adhesion Energies of Au, Cu, and Ag Nanoparticles on CeO₂(111), MgO(100) and Other Oxide Surfaces**, *Charles T. Campbell, S.L. Hemmingson, G.M. Feeley*, University of Washington

Heterogeneous catalysts consisting of late transition metal nanoparticles dispersed across oxide supports are ubiquitous in industrial chemistry and energy technology. We have used an ultrahigh vacuum single-crystal adsorption calorimeter to study the adsorption energies of Au, Cu and Ag gas atoms as they adsorb and grow nanoparticles on single-crystal oxide surfaces as models for real catalyst systems. These measurements allow us to determine the chemical potential of metal atoms in supported nanoparticles as a function of particle size and the support upon which they sit. The support effect manifests itself very directly on metal chemical potential via the metal / oxide adhesion energy. Our earlier studies have shown that metal chemical potential can be related to the metal nanoparticle's catalytic activity and deactivation rates through sintering, so there is a great motivation to understand how it varies with particle size and support, and how metal / oxide adhesion energies vary with the nature of the metal and the oxide support material. Through these measurements on a variety of systems, we have discovered systematic trends in these that allow predictions of adhesion energies for system which have not been measured. We have also measured the adsorption energy of isolated Cu atoms on CeO₂(111) terrace sites, which is possible at 100 K. This is the first

measurement of the adsorption energy of any late transition metal atom on any oxide surface of the type used as catalyst supports in a situation where the atom sits on the surface as an isolated monomer (as opposed to sitting within a small metal cluster).

9:20am **SS2+AS+HC+NS-TuM5 Effects of Nanoparticles on Surface Resistivity: Ni on Au(111)**, *Joshua Cohen, R.G. Tobin*, Tufts University

The change in surface resistivity due to the formation of nickel nanoparticles on gold(111) was studied by measuring the resistance of a thin film of Au as a function of Ni coverage, θ . After annealing, Au(111) configures into the herringbone reconstruction and provides a template for the periodic nucleation and growth of Ni nanoparticles. The Ni islands grow radially until $\theta \sim 0.3$ ML, after which, subsequent Ni atoms contribute almost exclusively to a second layer [1].

Surface resistivity arises primarily from the scattering of the substrate's conduction electrons by foreign atoms or defects, and studies of the dependence of surface resistivity on coverage yield insights into growth dynamics, interadsorbate interactions, and interactions between the adsorbed atoms and conduction electrons. For randomly distributed non-interacting scatterers the resistivity change is linear in coverage. Since Ni atoms on Au(111) grow in tight ordered nanoclusters, a nonlinear dependence might be anticipated. Our results, however, show a linear dependence on coverage for Ni atoms in the first layer, as if they were independent point scatterers. At coverages above $\theta \sim 0.3$ ML, there is no further change in resistivity, which we attribute to Ni atoms forming a second layer and making no significant contribution to the surface resistivity.

The samples were 150 nm thick epitaxial Au(111) films on mica prepared by sputtering and annealing in ultrahigh vacuum. The resistance of the film was measured as Ni was thermally evaporated on the surface. Ni coverage was determined using Auger electron spectroscopy (AES), corrected for the inelastic mean free path of the electrons.

The resistance and AES data were analyzed in terms of a growth model that allowed for variation in the coverage at which a second layer begins, the relative probabilities of first- and second-layer growth after that point, and the relative contributions of first- and second-layer Ni atoms to the surface resistivity. The results are consistent with the growth model observed with STM [1], and serve as an indirect probe of the growth kinetics of this interesting system, as well as determining for the first time the contributions of the Ni islands to the surface resistivity of the Au film.

1. Chambliss, D.D., R.J. Wilson, and S. Chiang, *Ordered Nucleation of Ni and Au Islands on Au (111) Studied By Scanning Tunneling Microscopy*. Journal of Vacuum Science & Technology B, 1991. 9(2): p. 933-937.

9:40am **SS2+AS+HC+NS-TuM6 Three-Dimensional Control of Nanoparticle Layer Deposition by "Click Chemistry"**, *Mackenzie Williams, A.V. Teplyakov*, University of Delaware

Our previous studies have focused on the formation of highly-controlled nanoparticle mono- and multilayers of silica and magnetic iron oxide nanoparticles through the copper(I) catalyzed azide-alkyne cycloaddition reaction. By using the specific functionalization scheme in that method, we achieved very high surface coverage and the formation of exactly one nanoparticle layer per deposition cycle, as could be observed with scanning electron microscopy (SEM) and atomic force microscopy (AFM). Formation of the triazole ring from the "click" reaction was confirmed by infrared spectroscopy and X-ray photoelectron spectroscopy (XPS), while density functional theory calculations were used to confirm spectroscopic results and investigate the reasons behind the high coverage. In the current work, a higher level of control over the nanoparticle layers is being sought. Conformal filling of the layer over high aspect-ratio features is being studied and would allow this method to be used as a viable alternative to traditional layer-by-layer techniques. Additionally, control of the spatial resolution of the nanoparticle layers upon the substrate via alternative methods of catalysis initiation is currently being investigated.

11:00am **SS2+AS+HC+NS-TuM10 Spherical Metallic Nanostructures Based on Fullerene Scaffolds with Tunable Bandgap, A Scanning Tunneling Microscopy/Spectroscopy (STM/STS) Study**, *Ehsan Monazami*, University of Virginia; *J.B. McClimon*, University of Pennsylvania; *J.M. Rondinelli*, Northwestern University; *P. Reinke*, University of Virginia

The current literature on annealing of fullerene molecules on tungsten surfaces indicates a complete dissociation of the fullerene cage and the formation of a carbide phase. However, our measurements with high resolution STM and STS illustrate a complex intermediate reaction sequence. Upon annealing of C₆₀ adsorbed on a tungsten thin film grown

Tuesday Morning, November 8, 2016

on MgO (001) in UHV, C_{60} does not dissociate and the spherical C_{60} shape is retained up to a temperature of at least 973 K. During the annealing, the band gap of the molecular layer decreases gradually from the wide bandgap of fullerene to a fully metallic electronic state. This transition occurs in a narrow temperature range between 600 K and 700 K. After this transition, the near-spherical particles are termed "nanospheres." This progression was observed with a series of high resolution scanning tunneling spectra and detailed spectral mapping. The bandgap variation presents an approach to achieve the formation of densely packed nanoclusters (nanospheres) with variable bandgap, which are stable at elevated temperatures. Experimental results for sub-ML fullerene coverage on tungsten show that the fullerene molecules are mobile at room temperature, but they become stationary after annealing above 500 K. This immobilization of molecules indicates a strong interaction and likely a covalent bond between the molecule and substrate that is triggered by annealing.

The progression to metallic nanospheres is hypothesized to occur either by gradual substitution of W-atoms or by wetting the molecule with W-atoms and thus formation of W-C bonds in a solid state reaction. These models were tested using density functional theory (DFT) calculations. Two simulation strategies were used. In the first, C_{60} carbon atoms were substituted by W in the molecule and the resulting electronic properties and bandgap were calculated. In the second approach, different adsorption geometries of a C_{60} molecule on the tungsten (110) surface were considered. The variation of the band gap due to different C_{60} orientations relative to the tungsten substrate and various types of hetero-fullerenes will be discussed.

11:20am SS2+AS+HC+NS-TuM11 Facile Synthesis of Gold Nanoworms and their Excellent Surface Enhanced Raman Scattering (SERS) and Catalytic Properties, Waqar Ahmed, COMSATS Institute of Information Technology, Pakistan; *J.M. van Ruitenbeek*, Leiden University, Netherlands

Gold nanoparticles exhibit interesting optical properties because of the surface plasmon resonance. The shape and size of gold nanoparticles can markedly influence their optical properties. A spherical nanoparticle has a single plasmon peak, while rod-shaped nanoparticles have two plasmon peaks because of their shape anisotropy. Furthermore, slight deviations from the rod morphology can markedly influence the optical properties. For example, worm-shaped gold nanoparticles can have more than two plasmon peaks. Moreover, nanoworms can display very high local field enhancements upon plasmon excitation owing to their special shape and surface roughness.

We have devised a simple, seedless, high-yield protocol for the synthesis of gold nanoworms [1]. Nanoworms were grown simply by reducing $HAuCl_4$ with ascorbic acid in a high pH reaction medium in the presence of growth directional agents. In contrast to the seed-mediated growth of gold nanorods where a seed particle grows into a nanorod, nanoworms grew by oriental attachment of nanoparticles. By varying different reaction parameters we were able to control the length of NWs from a few nanometers to micrometers. Furthermore, the aspect ratio can also be tuned over a wide range.

Owing to their special morphology, gold nanoworms are much superior than the conventional nanorods for numerous applications. For instance, we have seen that they show markedly superior SERS and catalytic properties compared to their nanorod counterparts. This is due to their high-energy rough surface and twisted shape, which not only provides an ideal platform for catalytic activities but also generates local hot-spots upon plasmon excitation. Our study shows that both catalytic and SERS properties of gold nanoworms are strongly dependent on their length.

[1] W. Ahmed, C. Glass, and J.M. van Ruitenbeek, *Nanoscale*, 6, 13222, (2014)

11:40am SS2+AS+HC+NS-TuM12 Surface Hydrogen Enables Sub-Eutectic Vapor-Liquid-Solid Semiconductor Nanowire Growth, S.V. Sivaram, H. Hui, Georgia Institute of Technology; *M. de la Mata, J. Arbiol*, Catalan Institute of Nanoscience and Nanotechnology, Spain; **Michael Filler**, Georgia Institute of Technology

Semiconductor nanowires are emerging as indispensable nanoscale building blocks for next generation energy conversion, electronic, and photonic devices. The bottom-up vapor-liquid-solid (VLS) mechanism – whereby a liquid eutectic "catalyst" droplet collects precursor molecules (or atoms) from the vapor and directs crystallization of the solid nanowire – is a nearly ubiquitous method for nanowire synthesis. While VLS growth below the bulk metal-semiconductor eutectic temperature has long been known, the fundamental processes that govern this behavior are poorly

Tuesday Morning, November 8, 2016

understood. Here, we show that hydrogen atoms adsorbed on the Ge nanowire sidewall enable AuGe catalyst supercooling and control Au transport. Our experimental approach combines in situ infrared spectroscopy to directly and quantitatively determine hydrogen atom coverage with a "regrowth" step that allows catalyst phase to be determined with ex situ electron microscopy. Maintenance of a supercooled catalyst with only hydrogen radical delivery confirms the centrality of sidewall chemistry. This work underscores the importance of the nanowire sidewall and its chemistry on catalyst state, identifies new methods to regulate catalyst composition, and provides synthetic strategies for sub-eutectic growth in other nanowire systems. We leverage this newfound understanding of nanowire growth chemistry to fabricate large-area arrays of high quality axial Si/Ge heterostructures for the first time.

12:00pm SS2+AS+HC+NS-TuM13 Ultrafine Sodium Titanate Nanowires with Extraordinary Strontium Ion-Exchange Property, Koji Nakayama, Tohoku University, Japan

The removal of radioactive substances released to the environment by a nuclear accident is an emergent issue. The water treatment based on the ion exchange process is the most effective decontamination technology, and inorganic ion exchangers, titanates, have been used for the capture of Sr ions owing to their high radiation stability and extreme ion selectivity. However, the reported adsorption capacity and ion exchange efficiency are not satisfied. We show the formation of sodium titanate nanowires with a few nanometers in diameter, having a mogul-shaped surface, forming hierarchically a three-dimensional network skeletal structure, and exhibiting remarkable Sr ion exchange properties [1]. They are produced by unique and simple non-thermal processes through the simultaneous selective leaching of Al and oxidation of Ti in a rapidly solidified Ti-Al alloy ribbon in NaOH solution. The experimental saturated adsorption capacity is tripled and the uptake rate is at least three hundred times faster than these of the previous reports. The results demonstrate that the newly created nanowires exhibit a potential application in the decontamination and disposal of nuclear waste.

[1] Y. Ishikawa, S. Tsukimoto, K. S. Nakayama, and N. Asao, *Nano Lett.* **15**, 2980-2984 (2015).

Surface Science

Room 104D - Session SS+HC-TuA

Photocatalysis and Photochemistry at Surfaces

Moderator: Arthur Utz, Tufts University

2:20pm SS+HC-TuA1 Investigations of Surface Chemistry for Pyridine-catalyzed CO₂ Reduction on GaP, C.X. Kronawitter, Bruce Koel, Princeton University

The surface chemistry of N-containing heteroaromatics, molecular co-catalysts that enable the selective electrochemical reduction of CO₂ to fuels, is discussed. The presented experimental results focus on elucidating the role of the electrode surface in CO₂ reduction reactions that are co-catalyzed by pyridine. For this catalysis, exceptionally high selectivity for reduced fuels has been reported when the reaction occurs at the surface a GaP photocathode. For this reason, experimental emphasis is placed on assessing preferential adsorption sites and bonding interactions of adsorbates on surfaces of GaP. A surface science approach is used, whereby ultra-high vacuum conditions facilitate the fabrication of highly characterizable electrode-adsorbate systems. The use of single crystal surfaces permits analysis of surface chemistry independent of complicating factors such as grain boundaries and morphology. Surface-sensitive core-level and vibrational spectroscopy techniques, including high-resolution X-ray photoelectron spectroscopy, synchrotron-based photoemission, and high-resolution electron energy loss spectroscopy, are used to probe adsorbate-substrate and adsorbate-adsorbate interactions for pyridine, water, hydrogen, and carbon dioxide on GaP. Scanning tunneling microscopy was used to obtain molecular orbital-resolved images of adsorbed molecules. Conclusions from experimental results on these model systems are supported by calculations using density functional theory. This work assists in generating a molecular-level understanding of the heterogeneous processes important to the reaction mechanisms involved in the efficient photoelectrocatalytic generation of carbon-containing fuels with high energy densities.

2:40pm SS+HC-TuA2 Photoreactivity of Benzoate Monolayers on TiO₂: Comparison of Anatase (001) and Rutile (110), Erik Skibinski, W.J.I. DeBenedetti, A. Song, A. Ortoll-Bloch, M.A. Hines, Cornell University

The photoreactivity of organic self-assembled monolayers (SAMs) on TiO₂ surfaces is of considerable importance to applications such as dye-sensitized solar cells and photocatalytic environmental remediation. Despite extensive research, there remains little information about the reactivity of well characterized TiO₂ surfaces under ambient conditions. Here, we study the surface structure and photoreactivity of near-ideal benzoate monolayers prepared from dilute aqueous solutions and reacted at atmospheric pressure on anatase (001) and rutile (110) surfaces using scanning tunneling microscopy, infrared and x-ray photoelectron spectroscopies, and density functional theory.

We show that self-assembled monolayers of benzoate, an analogue of the organic linkage used in dye-sensitized solar cells, undergo rapid photodecomposition on both rutile (110) and anatase (001) under ultraviolet illumination in ambient and oxygen-rich conditions. Interestingly, while the two surfaces have similar, although not identical, reactivities, they differ in their reaction products, with the anatase polymorph producing a surface-bound ketene.

3:00pm SS+HC-TuA3 Light-driven H₂ Generation using Multicomponent Semiconductor-metal Colloidal Nanorod Heterostructures, Tianquan Lian, Emory University

INVITED

Quantum confined semiconductor nanocrystals have been widely investigated as light harvesting and charge separation components in photovoltaic and photocatalytic devices. The efficiency of these semiconductor nanocrystal-based devices depends on many processes, including light harvesting, carrier relaxation, charge separation and charge recombination. The competition between these processes determines the overall solar energy conversion (solar to electricity or fuel) efficiency. Compared with single component quantum dots (QDs), semiconductor nanoheterostructures, combining two or more materials, offer additional opportunities to control their charge separation properties by tailoring their compositions and dimensions through relative alignment of conduction and valence bands. Further integration of catalysts (heterogeneous or homogeneous) to these materials form multifunctional nanoheterostructures. Using CdSe/CdS/Pt, dot-in-rod nanorods (NRs) with Pt tips, as a model system, we are examining the mechanism of long-lived

charge separation and H₂ generation in the presence of sacrificial electron donor. The rates of electron transfer, hole transfer and charge recombination are directly monitored by transient absorption and time-resolved fluorescence spectroscopy. In this talk, we will discuss the mechanism of exciton dissociation, the dependence of the rates of elementary charge transfer processes on the dimension (size and length) and band alignment in these materials, and how these rates affect the overall H₂ generation efficiency.

4:20pm SS+HC-TuA7 Quenching of Electron Transfer Reactions through Coadsorption: A Study of Oxygen Photodesorption from TiO₂(110), Greg Kimmel, N.G. Petrik, M. Shen, M.A. Henderson, Pacific Northwest National Laboratory

Using temperature programmed desorption (TPD) and photon stimulated desorption (PSD), we show that coadsorbates of varying binding energies on the rutile TiO₂(110) surface exert a commensurate inhibiting influence on the hole-mediated photodesorption of adsorbed O₂. A variety of coadsorbates (Ar, Kr, Xe, N₂, CO, CO₂, CH₄, N₂O, acetone, methanol or water) were shown to quench O₂ photoactivity, with the extent correlating with the coadsorbate's gas phase basicity, which in turn determines the strength of the coadsorbate-Ti⁴⁺ bond. Coadsorbed rare gases inhibited the photodesorption of O₂ by ~10-25%, whereas strongly bound species (water, methanol and acetone) nearly completely inhibited O₂ PSD. We suggest that coadsorption of these molecules inhibit the arrival probability of holes to the surface. Band bending effects, which vary with the extent of charge transfer between the coadsorbate and the TiO₂(110) surface, are not expected to be significant in the cases of the rare gases and physisorbed species. These results indicate that neutral coadsorbates can exert a significant influence on charge transfer events by altering the interfacial dipole in the vicinity of the target molecule.

4:40pm SS+HC-TuA8 Different Effects of Oxygen Adsorption on the Band Bending of TiO₂ Nanoparticles Studied by Photoluminescence Spectroscopy, Shiliang Ma, M. Reish, Z. Zhang, I. Harrison, J.T. Yates, Jr., University of Virginia

By employing photoluminescence (PL) spectroscopy, it was found that oxygen adsorption on powdered TiO₂ changes the band bending of anatase in different ways. On the one hand, oxygen exposure leads to molecular chemisorption of oxygen molecules, which take up negative charge, but can be reversibly removed by ultraviolet photodesorption from the TiO₂ surface. Molecular chemisorption of oxygen molecules increases the upward band bending of TiO₂ and decreases the PL emission. On the one hand, oxygen can adsorb through irreversible reaction with defects, which occurs through an intermediate state of molecularly chemisorption, reducing the intrinsic upward band bending at the TiO₂ surface resulting in PL emission increase. Since band bending plays an important role in charge carrier migration to the surface, this finding that oxygen adsorption can have two different effects on the band bending of TiO₂ provides a new perspective on how oxygen and oxygen vacancies may modulate photocatalytic reaction efficiencies.

5:00pm SS+HC-TuA9 Imaging Photodecomposition of Trimethyl Acetic Acid on Cross-linked (1 × 2) Rutile TiO₂(110), Y. Xia, K. Zhu, Zhenrong Zhang, K.T. Park, Baylor University

Photoreactivity of reduced TiO₂ is important in photocatalytic applications. Cross-linked (1 × 2) rutile TiO₂(110) has been extensively studied, yet the exact atomistic model remains a point of contention. Employing a carboxylic acid as a probing molecule, we studied the structure of cross-linked (1 × 2) TiO₂(110) through the interaction of trimethyl acetic acid (TMAA) with various sites on the surfaces using *in situ* scanning tunneling microscopy (STM). We compared three specific atomistic models for (1 × 2) reconstructed TiO₂(110), Ti₂O₃, Ti₂O, and Ti₃O₆. The adsorption of TMAA on strands at room temperature strongly supports the Ti₂O model for cross-linked (1 × 2) reconstructed TiO₂(110). Photodecomposition of TMAA shows the dependence on the initial TMA coverage and O₂ pressure.

5:20pm SS+HC-TuA10 Non-Fullerene Acceptors for Organic Photovoltaics: PTCDA versus C₆₀, Steven Robey, National Institute of Standards and Technology

Extensive development of new polymer and small molecule donors has helped produce a steady increase in the efficiency of organic photovoltaic (OPV) devices. However, OPV technology would benefit from the introduction of non-fullerene acceptors. Unfortunately, efforts to replace fullerenes have typically led to significantly reduced efficiencies. A number of possible explanations for reduced efficiencies with non-fullerene acceptors compared to fullerene acceptors have been suggested, including

the formation of unfavorable morphologies in non-fullerene systems and/or favorable excitation/carrier delocalization in fullerenes. In addition, enhanced exciton dissociation associated with fundamental characteristics of the fullerene molecular electronic states has also been suggested. We employed time-resolved two-photon photoemission (TR-2PPE) to directly compare exciton dissociation at interfaces between zinc phthalocyanine (ZnPc) interfaces and the non-fullerene acceptor, perylene tetracarboxylic dianhydride (PTCDA) versus dissociation measured at the analogous interface with C₆₀, and thus help discriminate between these potential explanations. Exciton dissociation rates are comparable for phthalocyanine interfaces with both acceptors, allowing us to suggest a hierarchy for effects influencing higher efficiencies with fullerene acceptors.

5:40pm **SS+HC-TuA11 Use of Photoluminescence to Monitor Surface Chemistry of Metal Oxide Nanoparticles**, *S. Kim, D. Somaratne, James Whitten*, University of Massachusetts Lowell

Many metal oxides nanoparticles are photoluminescent upon irradiation with ultraviolet light, with visible emission arising from surface states and surface defects. Because of the sensitivity of the surface to adsorption and electron transfer to and from even weakly adsorbed molecules, photoluminescence (PL) is proving to be a convenient method of monitoring chemisorption and physisorption. Experimental and theoretical results are presented related to adsorption of various gases and organic vapors on zinc oxide, zirconium oxide, and titanium dioxide nanoparticles toward the goal of correlating adsorption to PL changes. X-ray and ultraviolet photoelectron spectroscopy (XPS and UPS) and Raman spectroscopy measurements have been performed on metal oxide nanoparticles and single crystals to investigate whether chemisorption occurs at room temperature and the details of adsorbate bonding. These results are combined with density functional theory (DFT) calculations to understand how adsorption influences the PL changes. In addition to atmospheric gases, examples of adsorbates that have been examined include ammonia, methanethiol, methanol, benzene, and pyridine. This research provides a convenient method of monitoring adsorption and lays the foundation for optochemical sensing, in which metal oxides may serve as a new type of gas sensor.

6:00pm **SS+HC-TuA12 Exploring Pd Adsorption, Diffusion, Permeation, and Nucleation on Bilayer SiO₂/Ru as a Function of Hydroxylation and Precursor Environment: From UHV to Catalyst Preparation**, *William Kaden*, University of Central Florida

The hydroxylation-dependent permeability of bilayer SiO₂ supported on Ru(0001) was investigated by XPS and TDS studies in a temperature range of 100 K to 600 K. For this, the thermal behavior of Pd evaporated at 100 K, which results in surface and sub-surface (Ru-supported) binding arrangements, was examined relative to the extent of pre-hydroxylation. Samples containing only defect-mediated hydroxyls showed no effect on Pd diffusion through the film at low temperature. If, instead, the concentration of strongly bound hydroxyl groups and associated weakly bound water molecules was enriched by an electron-assisted hydroxylation procedure, the probability for Pd diffusion through the film is decreased via a pore-blocking mechanism. Above room temperature, all samples showed similar behavior, reflective of particle nucleation above the film and eventual agglomeration with any metal atoms initially binding beneath the film. When depositing Pd onto the same SiO₂/Ru model support via adsorption of [Pd(NH₃)₄]Cl₂ from alkaline (pH 12) precursor solution, we observe notably different adsorption and nucleation mechanisms. The resultant Pd adsorption complexes follow established decomposition pathways to produce model catalyst systems compatible with those created exclusively within UHV despite lacking the ability to penetrate the film due to the increased size of the initial Pd precursor groups.

Fundamental Discoveries in Heterogeneous Catalysis Focus Topic

Room 103A - Session HC+SS-WeM

Bridging Gaps in Heterogeneously-catalyzed Reactions

Moderator: Ashleigh Baber, James Madison University

8:00am **HC+SS-WeM1 Vinyl Acetate Formation Pathways and Selectivity on Model Metal Catalyst Surfaces**, *Theodore Thuening*, University of Wisconsin-Milwaukee

Surface reaction pathways are explored on model single crystal catalyst surfaces using a combination of surface science experiments in ultrahigh vacuum, in-situ monitoring of the surface intermediates during reaction, and by using density functional theory (DFT) calculations. This approach enables detailed reaction pathways to be obtained and is illustrated using palladium catalyzed synthesis of vinyl acetate monomer (VAM). It is shown that vinyl acetate is formed on a Pd(111) and Pd(100) model catalysts via the so-called Samanos pathway, where reaction is initiated by coupling between ethylene and surface acetate species to form an acetoxyethyl intermediate that decomposes by β -hydride elimination to form VAM. The way in which adsorbate coverage affects both reactivity and selectivity is discussed.

8:20am **HC+SS-WeM2 In situ Monitoring of Acetylene Hydrogenation over a Pd/Cu(111) Single Atom Alloy Surface with Polarization Dependent Infrared Spectroscopy**, *Christopher M. Kruppe, J.D. Krooswyk, M. Trenary*, University of Illinois at Chicago

Low coverages of catalytically active metals deposited onto less active metal surfaces can form single atom alloys (SAAs), which often display unique catalytic properties. Such alloys are particularly attractive for selective hydrogenation reactions. It is therefore of interest to probe the surface structure and chemistry of such alloys in the presence of gas phase reactants. We have used polarization dependent reflection absorption infrared spectroscopy (PD-RAIRS) to monitor the in situ hydrogenation of acetylene to ethylene over a Pd/Cu(111) SAA surface. The coverage and morphology of the deposited Pd is elucidated with Auger spectroscopy (AES), temperature programmed desorption (TPD) of H_2 , and PD-RAIRS of CO. After exposing clean Cu(111) and Cu(111) with various Pd coverages to 10 L CO at 100 K, the RAIR spectra show that the surface is largely unchanged by the presence of less than 0.5 ML of Pd. In the presence of 1×10^{-2} Torr of CO at 300 K, significant CO coverages are only achieved when Pd is present on the surface. The Pd coverage determined from the areas of the CO peaks in the PD-RAIR spectra is approximately equal to the Pd coverage calculated from peak-to-peak ratios in the Auger spectra. Surface species and gas phase products of C_2H_2 hydrogenation are monitored between 180 K and 500 K on clean Cu(111) and Pd/Cu(111). With a total pressure of 1 Torr and a $C_2H_2:H_2$ ratio of 1:100, annealing a SAA-Pd/Cu(111) surface to 360 K results in complete conversion of all gas phase C_2H_2 to gas phase ethylene (C_2H_4), without producing any gas phase ethane (C_2H_6). The results demonstrate the utility of PD-RAIRS for monitoring the selective hydrogenation of acetylene to ethylene.

8:40am **HC+SS-WeM3 Novel in Situ Techniques for Studies of Model Catalysts**, *Edvin Lundgren*, Lund University, Sweden **INVITED**

Motivated mainly by catalysis, gas-surface interaction between single crystal surfaces and molecules has been studied for decades. Most of these studies have been performed in well-controlled environments, and has been instrumental for the present day understanding of catalysis. We have in recent years explored the possibilities to perform experiments at conditions closer to those of a technical catalyst, in particular at increased pressures. In this contribution, results from catalytic CO oxidation over Pd single crystal surfaces using High Pressure X-ray Photo emission Spectroscopy (HPXPS), Planar Laser Induced Fluorescence (PLIF), and High Energy Surface X-Ray Diffraction (HESXRD) will be presented.

Armed with structural knowledge from ultra-high vacuum experiments, the presence of adsorbed molecules and gas-phase induced structures can be identified, and related to changes in the reactivity and/or to reaction induced gas-flow limitations. The strength and weaknesses of the experimental techniques will be discussed.

9:20am **HC+SS-WeM5 Metastable Cluster Formation and Polymorphism of Hydrogen-bonding Molecules on Gold are a Consequence of the Pulse-deposition of a Solution into Vacuum**, *Ryan Brown, S.A. Kandel*, University of Notre Dame

A primary motivation in studying the assembly of molecules at an interface is to determine the underlying principles which drive the spontaneous formation of supramolecular structures under specific environmental conditions, with the ultimate goal being an understanding which allows control over such processes. Recently we have postulated the importance of solution-phase cluster formation during the pulse-deposition, in vacuum, of small organic and organometallic molecules which contain strong hydrogen bonding components, namely carboxylic acid functional groups, in addition to weak hydrogen bonding donors. Specifically, we have studied the cluster formation of 1,1'-ferrocenedicarboxylic acid, $Fc(COOH)_2$, which has been pulse deposited on Au(111)-on-mica substrates. We employed low temperature scanning tunneling microscopy (LT-STM) to observe which molecular clusters persist at the interface following pulse-deposition from solution. We subsequently performed annealing experiments to determine which of these species represent stable conformations, and which are metastable species formed in the solution droplet during deposition. LT-STM images of $Fc(COOH)_2$ show a coexistence between dimer, chiral hexamer, and square tetramer clusters. Since the bulk crystal structures for $Fc(COOH)_2$ are all comprised entirely of molecular dimers, the most stable 2D supramolecular structure likely is some array of dimers, whereas the other species present are metastable. We attribute the initial strong presence of metastable species to the formation of clusters in solution, followed by their precipitation as predicted by Ostwald's rule, then their adsorption on to the substrate in a kinetically-trapped conformation. Electrospray ionization mass spectrometry (ESI-MS) of $Fc(COOH)_2$ solutions supports the presence of hexamer clusters in solvent droplets, which confirms the possibility that the chiral hexamers observed after deposition precipitate from the solution droplet. Sequential mild annealing steps of this surface results in the formation of linear rows of square tetramers, chiral dimer domains, and eventually tilted dimer arrays. The prevalence of each of these species is related to the surface's thermal history, and this is characteristic of a system evolving under kinetic control. We propose that injection of solution into a vacuum environment can be exploited to produce supramolecular 2D-structures not observed in the bulk crystal, and that the frequency of nature of the metastable species present should be dependent on variables such as the solution concentration, solvent, and droplet size.

9:40am **HC+SS-WeM6 Understanding the Activity of Pt-Re Bimetallic Clusters on Titania and Pt-Re Alloy Surfaces in the Water Gas Shift Reaction**, *Donna Chen, A.S. Duke, K. Xie, A.J. Brandt, T.D. Maddumapatabandi*, University of South Carolina

The chemical activities of bimetallic Pt-Re clusters supported on $TiO_2(110)$ and single-crystal Pt-Re alloy surfaces are investigated as model systems for understanding Pt-Re catalysts in the water gas shift (WGS) reaction. The activities of these Pt-Re bimetallic surfaces are studied in a microreactor coupled to an ultrahigh vacuum chamber so that the surfaces can be characterized by X-ray photoelectron spectroscopy (XPS) before and after reaction. Bimetallic clusters consisting of a Re core covered by a Pt shell have turnover frequencies that are almost twice as high as that of the pure Pt clusters at 160 °C. Furthermore, the Re in the active bimetallic clusters remains in its metallic state because Re is not readily oxidized when it remains subsurface; there is no evidence that ReO_x is active in promoting the WGS reaction. Pure Re clusters are not active for the WGS reaction, and bimetallic clusters with significant Re at the surface are less active than pure Pt clusters. Surface Re is oxidized under reaction conditions and sublimates as Re_2O_7 . Post-reaction infrared spectroscopy studies show that CO and hydroxyls are detected on the surface.

11:00am **HC+SS-WeM10 Fundamental Studies of the Water-gas Shift and CO_2 Hydrogenation on Metal/oxide Catalysts: From Model Systems to Powders**, *Jose Rodriguez*, Brookhaven National Laboratory **INVITED**

In this talk, it will be shown how a series of *in-situ* techniques {X-ray diffraction (XRD), pair-distribution-function analysis (PDF), X-ray absorption spectroscopy (XAS), environmental scanning tunneling microscopy (ESTM), infrared spectroscopy (IR), ambient-pressure X-ray photoelectron spectroscopy (AP-XPS)} can be combined to perform detailed studies of the structural, electronic and chemical properties of metal/oxide catalysts used for the production of hydrogen through the water-gas shift reaction ($WGS, CO + H_2O \rightarrow H_2 + CO_2$) and the hydrogenation of CO_2 to methanol ($MS, CO_2 + 3H_2 \rightarrow CH_3OH + H_2O$). Under reaction conditions most WGS and MS

catalysts undergo chemical transformations that drastically modify their composition with respect to that obtained during the synthesis process. The active phase of catalysts which combine Cu, Au or Pt with oxides such as ZnO, CeO₂, TiO₂, CeO_x/TiO₂ and Fe₂O₃ essentially involves nanoparticles of the reduced noble metals. The oxide support undergoes partial reduction and is not a simple spectator, facilitating the dissociation of water, or the adsorption of CO₂, and in some cases modifying the chemical properties of the supported metal. Therefore, to optimize the performance of these catalysts one must take into consideration the properties of the metal-oxide interface. IR and AP-XPS have been used to study the reaction mechanism for the WGS and MS on the metal/oxide catalysts. Data of IR spectroscopy indicate that formate species are not necessarily involved in the main reaction path for these reactions on Cu-, Au- and Pt-based catalysts. Thus, a pure redox mechanism or associative mechanisms that involve either carbonate-like (CO₃, HCO₃) or carboxyl (HOCO) species should be considered. In the last two decades, there have been tremendous advances in our ability to study catalytic materials under reaction conditions and we are moving towards the major goal of fully understanding how the active sites for the production of hydrogen through the WGS or the hydrogenation of CO₂ to methanol actually work.

11:40am **HC+SS-WeM12 The Use of EC-STM to Study the Chemical Reactivity and Nanoscale Structure of Metal Surfaces**, A. Phillips, L. Jackson, H. Morgan, G. Jones, **Erin Iski**, University of Tulsa

In the development of surfaces as efficient catalysts, it is critical to understand and control the surface reactivity in a defined manner. Electrochemical Scanning Tunneling Microscopy (EC-STM) is an advantageous technique in that in addition to providing a local probe of the atomic surface structure, EC-STM also functions as a 3-electrode cell in which redox chemistry can be performed to harness the chemical reactivity of the surface. This technique offers a unique window to study catalysis at conditions outside of a UHV environment, specifically at ambient temperatures and in liquids. Also, cyclic voltammograms (CVs) can be generated to provide specific information regarding the nature of the redox events occurring at the surface. Within this framework, it is possible to study how certain surfaces can become activated and/or deactivated as a result of electrochemical manipulation. One specific example of a thermally deactivated surface is a single Ag layer on a Au(111) crystal. The Ag layer is deposited on the Au(111) surface using Underpotential Deposition (UPD), which is an extremely controllable electrochemical technique for the application of a monolayer (or less) of a metal onto a more noble metal. Surprisingly, this atomically-thin Ag layer when formed in the presence of halides remains on the Au surface after heat treatments as high as 1,000 K. Importantly, thermal stabilization can be contrasted and compared with catalytic activity in which chlorine has shown to be a promoter of ethylene epoxidation over Ag(111), demonstrating why this system is intriguing from multiple vantage points. From a general standpoint, EC-STM offers an environmentally unique handle on how the chemical reactivity of a metal surface can be altered and how that surface can then be studied on a fundamental level.

12:00pm **HC+SS-WeM13 Formation and Stability of Surface Oxides on Ag(111)**, **Daniel Killelea**, J. Derouin, R.G. Farber, M.E. Turano, Loyola University Chicago; E.V. Iski, The University of Tulsa

A long-standing challenge in the study of heterogeneously catalyzed reactions on silver surfaces has been the determination of what surface phases are of greatest chemical importance. This is due to the coexistence of several different surface phases on oxidized silver surfaces. A further complication is subsurface oxygen (O_{sub}). O_{sub} are O atoms dissolved into the near surface of a metal, and are expected to alter the surface in terms of chemistry and structure, but these effects have yet to be well characterized. We studied oxidized Ag(111) surfaces after exposure to gas-phase O atoms with a combination of surface science techniques to determine the resultant surface structure; we observed that once 0.1 ML of O_{sub} has formed, the surface dramatically, and uniformly, reconstructs to a striped phase at the expense of all other surface phases. Furthermore, O_{sub} formation is hindered at temperatures above 500 K. We also observed a coexistence of several surface oxides at intermediate deposition temperatures, and the predominance of the *p*(4x5v3) surface reconstruction at elevated temperatures.

Fundamental Discoveries in Heterogeneous Catalysis Focus Topic

Room 103A - Session HC+NS+SS-WeA

Nanoscale Surface Structures in Heterogeneously Catalyzed Reactions

Moderator: Arthur Utz, Tufts University

2:20pm **HC+NS+SS-WeA1 Ceria Nanoclusters on Graphene/Ru(0001): A New Model Catalyst System**, Z. Novotny, Pacific Northwest National Laboratory; F.P. Netzer, Karl-Franzens University, Austria; **Zdenek Dohnalek**, Pacific Northwest National Laboratory **INVITED**

Cerium oxide is an important catalytic material known for its ability to store and release oxygen, and as such, it has been used in a range of applications, both as an active catalyst and as a catalyst support. Using scanning tunneling microscopy and Auger electron spectroscopy, we investigated the growth of ceria nanoclusters and their oxygen storage/release properties on single-layer graphene (Gr) on Ru(0001) with a view towards fabricating a stable system for model catalysis studies. The ceria nanoclusters are of the CeO₂(111)-type and are anchored at the intrinsic defects of the Gr surface and display a remarkable stability against reduction in ultrahigh vacuum up to 900 K, but some sintering of clusters is observed for temperatures > 450 K. The evolution of the cluster size distribution suggests that the sintering proceeds via a Smoluchowski ripening mechanism, i.e. diffusion and aggregation of entire clusters. To follow the cluster redox properties we examined their oxygen storage and release in an oxygen atmosphere (<10⁻⁶ Torr) at elevated temperature (550 – 700 K). Under oxidizing conditions, oxygen intercalation under the Gr layer is observed. Time dependent studies demonstrate that the intercalation starts in the vicinity of the CeO_x clusters and extends until a completely intercalated layer is observed. Atomically resolved images further show that oxygen forms a p(2x1) structure underneath the Gr monolayer. Temperature dependent studies yield an apparent kinetic barrier for the intercalation of 1.2 eV. At higher temperatures, the intercalation is followed by a slower etching of the intercalated Gr (apparent barrier of 1.6 eV). Vacuum annealing of the intercalated Gr leads to the formation of carbon monoxide and causing etching of the Gr film thus revealing that the spillover of oxygen is not reversible. These studies demonstrate that the easily reducible CeO_x clusters act as intercalation gateways capable of efficiently delivering oxygen underneath the Gr layer.

3:00pm **HC+NS+SS-WeA3 Lowering the Barrier to C-H Activation using Pt/Cu Single Atom Alloys**, Matthew Marcinkowski, M. El Soda, F.R. Lucci, E.C.H. Sykes, Tufts University

Due to the increased in shale gas production in recent years the availability of light alkanes such as ethane and propane has increased significantly. Although these chemicals are typically considered inert, the ability to cleave C-H bonds in alkanes would allow for production of alkenes, which are important precursors to polymers. In this work, we use a surface science approach to model C-H activation on a Cu(111) surface using methyl iodide. Methyl iodide is known to decompose to produce methyl groups and iodine atoms on Cu(111) below 200 K. The methyl groups are then stable on the surface up until 450 K, at which temperature they decompose to form a number of products including methane, ethylene, ethane, and propylene. The rate limiting step to forming these products is the activation of one of the C-H bonds in the methyl group to produce surface bound hydrogen and methylene. Pt(111) is also able to activate the C-I bond in methyl iodide, but methyl groups on this surface only produce methane, hydrogen, and surface bound methylene groups at 290 K. While the barrier to C-H activation is lowered on Pt compared to Cu, the Pt surface is unable to perform carbon coupling reactions. Inspired by these previous results, we fabricated surfaces consisting of 1% Pt in the Cu(111) surface. At this concentration, Pt exists as single, isolated atoms substituted into the Cu(111) lattice. These *single atom alloys* exhibit synergistic chemistry and yield the desirable properties of each of the two pure metal surfaces. They are able to produce carbon coupling products like pure Cu, but are able to activate the C-H bond necessary to begin these reactions at 340; 110 K cooler than on Cu(111). Increasing the concentration of Pt further decreases the temperature necessary to activate C-H bonds, but also decreases the amount of carbon coupling products formed as the surface becomes more similar to Pt(111). Single atom alloys therefore provide an ideal model catalyst for the decomposition of methyl iodide, allowing for more facile activation of the

C-H bond than pure Cu while also producing the desired coupling products, which Pt(111) is unable to do.

3:20pm **HC+NS+SS-WeA4 Formation, Migration and Reactivity of Au-CO Complexes on Gold-Surfaces**, Jun Wang, Oak Ridge National Laboratory; M. McEntee, W. Tang, M. Neurock, University of Virginia; A.P. Baddorf, P. Maksymovych, Oak Ridge National Laboratory; J.T. Yates, Jr., University of Virginia

We report experimental as well as theoretical evidence that suggests formation of Au-CO complexes upon the exposure of CO to active sites (step edges and threading dislocations) on a Au(111) surface. Room-temperature scanning tunneling microscopy (STM), X-ray photoelectron spectroscopy, transmission infrared spectroscopy, and density functional theory calculations point were combined to investigate morphological changes of the Au(111) surface with an intentionally created array of etch-pits. Room-temperature STM of the Au(111) surface at CO pressures in the range from 10⁻⁸ to 10⁻⁴ Torr (dosage up to 10⁶ langmuir) indicates Au atom extraction from dislocation sites of the herringbone reconstruction, mobile Au-CO complex formation and diffusion, and Au adatom cluster formation on both elbows and step edges on the Au surface. The formation and mobility of the Au-CO complex result from the reduced Au-Au bonding at elbows and step edges leading to stronger Au-CO bonding and to the formation of a more positively charged CO (CO^{δ+}) on Au. Our studies indicate that the mobile Au-CO complex is involved in the Au nanoparticle formation and reactivity, and that the positive charge on CO increases due to the stronger adsorption of CO at Au sites with lower coordination numbers.

ACKNOWLEDGEMENTS: Part of this research was conducted at the Center for Nanophase Materials Sciences (CNMS), which is a DOE Office of Science User Facility .

Reference: J. Wang, M. McEntee, W. Tang, M. Neurock, A. P. Baddorf, P. Maksymovych, and J. T. Yates, Jr., *J. Am. Chem. Soc.* 138, 1518 (2016)

4:20pm **HC+NS+SS-WeA7 Sulfur-Metal Complexes on Surfaces of Copper, Silver, and Gold**, Patricia A. Thiel, Iowa State University; H. Walen, RIKEN Surface and Interface Science Laboratory, Wako, Saitama, Japan; D.-J. Liu, Ames Laboratory, Ames, IA; J. Oh, RIKEN Surface and Interface Science Laboratory, Wako, Saitama, Japan; H.J. Yang, University College London, UK; Y. Kim, RIKEN Surface and Interface Science Laboratory, Wako, Saitama, Japan **INVITED**

The nature of sulfur interaction with surfaces of coinage metals (M=Cu, Ag, Au) is relevant to aspects of heterogeneous catalysis, corrosion, and self-assembled monolayers. We have discovered a number of unexpected complexes—-independent, molecule-like MxSy species—that form on low-index M surfaces. In a sense, these complexes are iidway between the well-known phenomena of chemisorption and adsorbate-induced reconstruction. Our primary experimental tool is scanning tunneling microscopy (STM) used in ultrahigh vacuum. We tailor our experimental conditions to isolate the complexes, by working at ultra-low sulfur coverage to avoid competition from surface reconstructions. Furthermore, we prepare the surface at 300 K, but image at 5 K, in order to immobilize these small species. Density functional theory (DFT) is used to interpret the experimental results. For instance, application of DFT is essential to identify the complexes that form on Cu(111), Ag(111), and Au(100), and this identification is made both on the basis of their physical characteristics in real vs. stimulated STM images (size, orientation, shape) as well as their calculated stability. On other surfaces, including Au(111), Cu(100), and Au(110), MxSy complexes do not form under comparable conditions. This broad database and extensive analysis provides insights into factors that favor complexation in this class of systems.

5:00pm **HC+NS+SS-WeA9 Titania/Gold Inverse Model Catalysts for Acetaldehyde Formation from Ethanol**, Ashleigh Baber, D.T. Boyle, W. Andahazy, V. Lam, D. Schlosser, N. Tosti, J. Wilke, James Madison University The fundamental investigation of the catalytic chemistry of ethanol at interfaces is important for many fields including the automotive industry due to the use of ethanol as a fuel. The redox chemistry of small alcohols, including methanol and propanol, has been studied on Au(111) supported TiO₂ nanoparticles, yet the active site for the chemistry has not yet been elucidated. Here, the systematic study of ethanol has been investigated on Au(111) and TiO₂/Au(111) via temperature programmed desorption in an effort to gain insight on the interfacial role of the reactivity for ethanol, as a function of titania coverage. Ex situ atomic force microscopy was used to image the gold-supported titania particles, and X-ray photoelectron spectroscopy was used to confirm the presence of titania on the surface.

Wednesday Afternoon, November 9, 2016

The presence of TiO₂ nanoparticles on Au(111), ~25 nm in diameter, led to the catalytic conversion of ethanol to acetaldehyde at temperatures greater than 400 K. The interaction of ethanol with Au(111)-supported TiO₂ nanoparticles is markedly different than its interaction with the individual counterparts: bulk titania and gold, which both lead to the desorption of molecular ethanol at temperatures lower than 400 K.

5:20pm HC+NS+SS-WeA10 Shape and Support Interaction of Size Selected Pt Nanoparticles in Presence of H₂, Mahdi Ahmadi, F. Behafarid, University of Central Florida; B. Roldan Cuenya, Ruhr-University Bochum, Germany
Pt nanoparticles (NPs) supported on TiO₂ have been widely used as catalysts in industrial applications.

Strong metal-support interaction (SMSI) is expected to occur for this system under reducing environments

such as vacuum and H₂. Since the morphology of NPs depends on their surface energy and their interaction

with the support, investigating the shape of NPs could be an excellent pathway to understand the metal

support interactions. In this study we have investigated the in situ shape evolution of TiO₂ supported Pt NP

using grazing incidence small angle X-ray scattering (GISAXS) during annealing in H₂ environment. The

size selected Pt NPs with an initial spherical shape were synthesized via inverse micelle encapsulation

method. The sample was step annealed up to 700°C in H₂ environment and the onset for NPs faceting was

found to be 600°C. Annealing at a higher temperature (700°C) did not cause any further change in NPs

structure. The presence of a sharp scattering ray at 45° with respect to the surface normal indicates the (110)

facet to be the dominant side facet for Pt NPs and the top and interfacial facets to be Pt(100). These features

point out that the shape of Pt NPs supported on TiO₂ under hydrogen environments is pyramidal. The

specific shape of Pt NPs are discussed based on the SMSI phenomenon.

5:40pm HC+NS+SS-WeA11 Single Atom Alloys as a Strategy for Selective Heterogeneous Hydrogenation and Dehydrogenation Reactions, Charles Sykes, Tufts University
INVITED

Catalytic hydrogenations are critical steps in many industries including agricultural chemicals, foods and pharmaceuticals. In the petroleum refining, for instance, catalytic hydrogenations are performed to produce light and hydrogen rich products like gasoline. Typical heterogeneous hydrogenation catalysts involve nanoparticles composed of expensive noble metals or alloys based on platinum, palladium, rhodium, and ruthenium. We demonstrated how single palladium and palladium atoms can convert the otherwise catalytically inert surface of an inexpensive metal into an ultraselective catalyst. (1-3) High-resolution imaging allowed us to characterize the active sites in single atom alloy surfaces, and temperature programmed reaction spectroscopy to probe the chemistry. The mechanism involves facile dissociation of hydrogen at individual palladium atoms followed by spillover onto the copper surface, where ultraselective catalysis occurs by virtue of weak binding. The reaction selectivity is in fact much higher than that measured on palladium alone, illustrating the system's unique synergy.

Our *single atom alloy* approach may in fact prove to be a general strategy for designing novel bi-functional heterogeneous catalysts in which a catalytically active element is atomically dispersed in a more inert matrix. Very recently we demonstrated that this strategy works in the design of real catalysts. Platinum/copper nanoparticles can perform the industrially important butadiene hydrogenation at lower temperature using just 1% platinum. (3) Moreover, some of the best industrial alloy catalysts to date may already be operating via this mechanism, but there is currently no method to directly probe the atomic geometry of a working catalyst. Our scientific approach allows one to parse out the minimal reactive ensembles in an alloy catalyst and provide design rules for selective catalytic nanoparticle. *From another practical application standpoint, the small amounts of precious metal required to produce single atom alloys generates a very attractive alternative to traditional bimetallic catalysts.*

References:

- 1) G. Kyriakou, M. B. Boucher, A. D. Jewell, E. A. Lewis, T. J. Lawton, A. E. Baber, H. L. Tierney, M. Flytzani-Stephanopoulos and E. C. H. Sykes - *Science* 2012, 335, 1209
- 2) M. D. Marcinkowski, A. D. Jewell, M. Stamatakis, M. B. Boucher, E. A. Lewis, C. J. Murphy, G. Kyriakou and E. C. H. Sykes - *Nature Materials* 2013, 12, 523
- 3) F. R. Lucci, J. Liu, M. D. Marcinkowski, M. Yang, L. F. Allard, M. Flytzani-Stephanopoulos, and E. C. H. Sykes - *Nature Communications* 2015, 6, 8550

In-Situ and Operando Spectroscopy and Microscopy for Catalysts, Surfaces, & Materials Focus Topic Room 101C - Session IS+HC-WeA

Ambient Pressure XPS Studies of Surface and Chemistry of Catalysts

Moderators: Franklin (Feng) Tao, University of Kansas, Anatoly Frenkel, Yeshiva University

2:20pm IS+HC-WeA1 The Electronic Structure of Electrochemically Active Interfaces, V. Pfeifer, Fritz-Haber-Institut der Max-Planck-Gesellschaft and Helmholtz-Zentrum Berlin, Germany; J.J. Velasco-Velez, Max-Planck-Institut für Chemische Energiekonversion, Germany; R. Arrigo, Diamond Light Source Ltd., UK; T.E. Jones, Fritz-Haber-Institut der Max-Planck-Gesellschaft, Germany; M. Hävecker, Max-Planck-Institut für Chemische Energiekonversion, Germany; E. Stotz, Fritz-Haber-Institut der Max-Planck-Gesellschaft, Germany; R. Schlögl, Fritz-Haber-Institut der Max-Planck-Gesellschaft and Max-Planck-Institut für chemische Energiekonversion, Germany; Axel Knop-Gericke, Fritz-Haber-Institut der Max-Planck-Gesellschaft, Germany
INVITED

In this presentation I will describe the application of near ambient pressure photoelectron spectroscopy (NAPXPS) to the investigation of electrochemically active gas-solid and liquid-solid interfaces during electrochemical processes. Understanding the oxygen evolution reaction (OER) on a molecular level has become increasingly important over the last few years, because energy storage of renewables is becoming more relevant now that CO₂ emission has been identified as a source of climate change.

Nafion membrane based NAPXPS experiments performed on Pt electrodes during the OER demonstrate that Pt oxides are detrimental for the OER. An oxygen induced species characterized by an Pt4f binding energy 0.6 eV above the metallic Pt4f peak was observed. However, these experiments were done in water vapor and the relevance of the results for the OER in liquid water is questionable [1]. Therefore a new approach to study the liquid-solid interface during an electrochemical process in liquid water was developed.

In this new process the electrode material is deposited on a bilayer of graphene that is stabilized by a silicon nitride window with a pinhole structure. The electrode is exposed to the aqueous electrolyte and is irradiated at the same time by synchrotron light through the bilayer graphene membrane. The emitted photoelectrons have to pass the graphene membrane before being detected in the photoelectron analyzer [2]. Recent progress in the study of the electronic structure of noble metal electrodes used in OER reaction will be discussed [3,4].

References:

1. R. Arrigo et al., In Situ Study of the Gas-Phase Electrolysis of Water on Platinum by NAP-XPS, *Angew. Chem. Int. Ed.* **52**, 11660-11664 (2013)
2. J. J. Velasco-Velez et al., Photoelectron spectroscopy at the graphene-liquid interface reveals the electronic structure of an electrodeposited cobalt/graphene electrocatalyst, *Angew. Chem. Int. Ed.* **54**, 14554-14558 (2015)
3. V. Pfeifer et al., The electronic structure of iridium oxide electrodes active in water splitting, *PCCP*, **18**, 2292-2296 (2016)
4. V. Pfeifer et al., The electronic structure of iridium and its oxides, *Surf. Interface Anal.*, **48**, 261-273 (2016)

3:00pm IS+HC-WeA3 In situ AP-XPS and NEXAFS Studies on CO Oxidation and CO₂ Dissociation on Copper Surfaces, B. Eren, Christian Heine, G.A. Somorjai, M.B. Salmeron, Lawrence Berkeley National Laboratory (LBNL)

This presentation contains three parts: 1- Surface science approach to CO oxidation reaction on the low-index Cu surfaces which shows at oxygen

lean conditions where the Cu surface is not oxidized to Cu₂O, (111) face of Cu is more active than more open (100) and (110) faces. This is due to high binding energy of atomic oxygen on Cu, i.e., poisoning of the lower coordinates sites of Cu. 2- Chemical state of the surface and subsurface, and adsorbate coverage on Cu(111) in steady state conditions. Here, we provide phase diagram of the surface under reaction conditions. Interestingly, no CuO phase occurs between 273K-413K when the CO:O₂ ratio is chosen as 2:1 or above. Cu₂O phase appears to be to more active phase, however it still unclear whether the reaction on Cu₂O is a MvK or LH type. 3- Finally, we present the chemical state and the surface morphology of Cu during CO₂ dissociation at ambient pressures, which appears to be different than in the presence of CO or O₂ alone.

3:20pm **IS+HC-WeA4 Alcohol Adsorption and Reaction on La_{0.7}Sr_{0.3}MnO₃(100) by APXPS, David Mullins, T.Z. Ward, S.H. Overbury, Oak Ridge National Laboratory**

Perovskite materials that are characterized by the composition ABO₃ can be formed by a wide variety of A and B cations. This enables the catalytic properties to be altered by selectively choosing the constituents while maintaining nominally the same structure. The adsorption and oxidation of simple alcohols such as methanol and ethanol have been identified as probe reactions to characterize and compare the catalytic properties of different oxide surfaces.

Methanol and ethanol oxidation on doped La_{0.7}Sr_{0.3}MnO₃(001) have been studied using ambient pressure x-ray photoelectron spectroscopy (APXPS). La_{0.7}Sr_{0.3}MnO₃(001) was grown on single crystal Nb-doped SrTiO₃(001) by pulse laser deposition. The growth of this film has been extensively characterized as a function of temperature, oxygen pressure and laser fluence in order to produce near ideal crystallinity and morphology in the film. The APXPS experiments were performed on the end station at the recently commissioned Beamline CSX-2 at NSLS II. In order to investigate the so-called "pressure gap" that may occur between reactions studied under vacuum conditions and at pressure approaching atmospheric pressure, experiments were conducted at nominally 10⁻⁵ torr and at 0.1 torr between 250° C and 350° C.

Methanol forms methoxy when adsorbed on the perovskite surface at 250° C. The surface coverage was four times greater at 0.1 torr compared to 10⁻⁵ torr. Methoxy was the only C-containing surface species observed at 10⁻⁵ torr with or without O₂. Methoxy was also the dominant surface species at 0.1 torr in the absence of O₂. However, small amounts of formate and atomic C were also evident. At the higher pressure the Mn 2p spectra indicated that the alcohol partially reduced Mn³⁺ to Mn²⁺. There was also an indication in the O 1s spectra that O was removed from the surface.

When O was present at 0.1 torr formate became the dominant surface species with only trace amounts of methoxy and C also evident. Gas phase CO₂ and H₂O products were also detected in the C 1s and O 1s spectra.

Results using ethanol rather than methanol as the reactant were generally the same, i.e. only ethoxy on the surface at lower pressures, a mixture of ethoxy and acetate at higher pressure in the absence of O₂, and exclusively acetate on the surface when O₂ was present. The only significant difference between methanol and ethanol was a greater tendency for ethanol to form the carboxylate in the absence of O₂.

Operando experiments are planned to monitor the products with a mass spectrometer to determine whether the different pressures, and resulting surface species, lead to different products.

5:00pm **IS+HC-WeA9 In situ Spectroscopy for Catalyst Design, Rosa Arrigo, Diamond Light Source, Oxfordshire, UK** **INVITED**

Observing structural dynamics of heterogeneous catalysts in action yields important mechanistic insights to guide the synthesis towards improved materials. Synchrotron-based ambient pressure X-ray photoemission spectroscopy (AP-XPS) has become very popular worldwide to serve this purpose.¹⁻³ One expanding field of application of this technique is electro-catalysis²⁻³ due to its central role in a renewable energy scenario. In this contribution, I will present two examples of the application of this technique to study the gas/solid interface of electro-catalysts for a polymeric electrolyte membrane-based electrode assembly.⁴ The first example is the oxygen evolution reaction (OER), which occurs at the anode side of an electrochemical cell for water electrolysis. Herein, the highly debated descriptions of the electronic structure of the oxygen evolving Pt⁴ and Ir⁵ surfaces are clarified. The second example is the CO₂ reduction reaction (CO₂RR) to fuel over Fe on N-functionalised carbon-based electro-catalysts. These catalysts proved to be active for the CO₂ reduction but the competing hydrogen evolution reaction (HER) from water reduction is

favoured. Results of this research will be presented which enable us to shine light onto the nature of the H evolving sites and CO₂ reducing sites on this type of catalyst.

[1] H. Bluhm, M. Hävecker, A. Knop-Gericke, M. Kiskinova, R. Schlögl, M. Salmeron, MRS Bulletin 32, 2007, 1022.

[2] J. J. Velasco-Velez, V. Pfeifer, M. Hävecker, R. S. Weatherup, R. Arrigo, C.-H. Chuang, E. Stotz, G. Weinberg, M. Salmeron, R. Schlögl, A. Knop-Gericke, Angewandte Chemie International Edition 54, 2015, DOI: 10.1002/anie.201506044.

[3] Z. Liu, H. Bluhm, Hard X-ray Photoelectron Spectroscopy (HAXPES), 447-466. DOI: 10.1007/978-3-319-24043-5_17.

[4] R. Arrigo, M. Hävecker, M. E. Schuster, C. Ranjan, E. Stotz, A. Knop-Gericke, R. Schlögl, Angewandte Chemie International Edition, 52, 2013, 11660-11664.

[5] V. Pfeifer, T. Jones, J.-J. Velasco-Velez, M. Greiner, C. Massué, R. Arrigo, D. Teschner, F. Girgsdies, M. Scherzer, J. Allan, M. Hashagen, G. Weinberg, S. Piccinin, M. Hävecker, A. Knop-Gericke, R. Schlögl, Physical Chemistry Chemical Physics 18, 2015, DOI: 10.1039/C5CP06997A.

5:40pm **IS+HC-WeA11 In Situ and Operando Characterization of Model Metal Nanoparticle Catalysts: Size, Shape, and Chemical State Effects, Beatriz Roldan Cuenya, Ruhr-University Bochum, Germany** **INVITED**

In order to comprehend the properties affecting the catalytic performance of metal nanoparticles (NPs), their dynamic nature and response to the environment must be taken into consideration. The working state of a NP catalyst might not be the state in which the catalyst was prepared, but a structural and/or chemical isomer that adapted to the particular reaction conditions. This talk provides examples of recent advances in the preparation and characterization of NP catalysts with well-defined sizes and shapes. It discusses how to resolve the shape of nm-sized Pt, Au, Pd, and Cu catalysts via a combination of *in situ* microscopy (AFM, STM, TEM), and *in situ* and *operando* spectroscopy (XAFS, GISAXS) and modeling, and how to follow its evolution under different gaseous or liquid chemical environments and in the course of a reaction. It will be highlighted that for structure-sensitive reactions, catalytic properties such as the reaction rates, onset reaction temperature, activity, selectivity and stability against sintering may be tuned through controlled synthesis.

Examples of catalytic processes which will be discussed include the gas-phase oxidation of alcohols (methanol, propanol, butanol), the oxidation and reduction of NO, the electrochemical oxidation of propanol and electrochemical reduction of CO₂. Emphasis will be given to elucidating the role of the NP size, shape and chemical state in the activity and selectivity of the former reactions.

Fundamental Discoveries in Heterogeneous Catalysis Focus Topic

Room 103A - Session HC+SS-ThM

Dynamics of Gas-surface Interactions in Heterogeneous Catalysis

Moderator: Daniel Killelea, Loyola University Chicago

8:00am **HC+SS-ThM1 Adsorption and Hydrogenation of Acrolein on Ru(001)**, *Dominic Esan*, *Y.D. Ren*, University of Illinois at Chicago; *I.B. Waluyo*, Brookhaven National Laboratory; *M. Trenary*, University of Illinois at Chicago

The partial hydrogenation of α , β -unsaturated aldehydes is an important step in several synthetic industrial processes especially in the fine chemicals and pharmaceutical industries. Generally, it has been established that the thermodynamics of the catalytic hydrogenation of these unsaturated aldehydes favor the formation of saturated aldehydes via the hydrogenation of the C=C bond while the manipulation of the kinetics of the process may yield the desired unsaturated alcohol product via the hydrogenation of the C=O bond. Most of the studies done on single metal surfaces using acrolein ($\text{CH}_2=\text{CH}=\text{CHO}$), the smallest of these aldehydes, show that the thermodynamically-preferred product (propanal) is always the favored product. However, bimetallic systems have been shown to possess unique properties, compared to their single metal counterparts, including novel reaction pathways. Thus, our aim is to study acrolein hydrogenation on a bimetallic Pt/Ru(001) system to determine if the presence of the Pt atoms can enhance the selectivity and activity towards the formation of the unsaturated alcohol (2-propenol).

In this initial study, temperature programmed desorption (TPD) and reflection absorption infrared spectroscopy (RAIRS) were used to determine if the bare Ru(001) surface is active towards (partial and complete) hydrogenation of acrolein and if it's selective for the desired product (2-propenol). At low coverages, acrolein was found to adsorb on the surface, at 90 K, via the C=O bond and completely decomposes to CO(g) around 460 K. As the coverage increases, adsorption via the C=C bond predominates and most of the acrolein desorbs molecularly or decomposes to CO(g). However, some of the acrolein also self-hydrogenates to yield all the possible hydrogenation products – propanal, 2-propenol, and 1-propanol with TPD peak temperatures at 180, 210, and 280 K respectively – with propanal having the highest yield. Co-adsorption with H_2 (g) enhances the adsorption via the C=C bond and the yield of all the products. These results will serve as a guide for the study on the Pt/Ru(001) system.

8:20am **HC+SS-ThM2 Dynamics of Formate Synthesis from CO_2 and Formate Decomposition on Cu Surfaces**, *J. Quan*, *T. Kozarashi*, *T. Ogawa*, *T. Kondo*, *Junji Nakamura*, University of Tsukuba, Japan

Much attention has been paid to methanol synthesis by hydrogenation of CO_2 as a promising chemical conversion of CO_2 . It has been well-known that Cu-based catalysts show high activity for the methanol synthesis, in which the initial elementary step of CO_2 is formation of formate species by the reaction of CO_2 with surface hydrogen atoms on Cu. Previous kinetic measurements of the formate synthesis by hydrogenation of CO_2 have suggested an Eley-Rideal (E-R) typed mechanism that CO_2 directly attacks a hydrogen atom on Cu surfaces. We have thus tried to prove the E-R typed mechanism by molecular beam experiments assuming that the reaction between incoming CO_2 molecules and Cu surfaces is thermally non-equilibrated. We first prepared hydrogen atoms on cold Cu(111), Cu(110), and Cu(100) kept around 200 K and then hot CO_2 molecular beams were illuminated onto the surfaces with controlling its vibrational and translational energy. It is found that the formate synthesis proceeds significantly without heating Cu samples if vibrational and translational energies are supplied to gaseous CO_2 . The results clearly indicate the thermal non-equilibrium dynamics. Possibility of a tunneling mechanism between CO_2 and a hydrogen atom on Cu was discarded because no significant H/D effect was observed on the reaction rate of formate synthesis. On the other hand, we have studied the dynamics of the formate decomposition as a reverse reaction of the formate synthesis. We measured the angular distribution and the translational energy of desorbed CO_2 formed by the decomposition of formate on Cu(110) under a steady state reaction of HCOOH and O_2 . The angular distribution showed a sharp collimation, $\cos^2\theta$, perpendicular to the surface. The translational energy of CO_2 was independent of the surface temperature of Cu(110). It is thus found that the formate decomposition is also thermal non-equilibrium

dynamics. However, the translational energy was as low as 100 meV, which is much lower than that required for formate synthesis, about 600 meV. The discrepancy will be discussed in the presentation.

8:40am **HC+SS-ThM3 Step-Type Selective Oxidation on Pt Surfaces**, *Rachael Farber*, Loyola University Chicago; *C. Badan*, Leiden Institute of Chemistry, The Netherlands; *H. Heyrich*, Leiden Institute of Chemistry; *L.B.F. Juurlink*, Leiden Institute of Chemistry, The Netherlands; *D.R. Killelea*, Loyola University Chicago

The development of predictive models of heterogeneously catalyzed systems relies on a sound understanding of the atomic-level details of the interactions of gas-phase species with the metal surface. A key factor in this tapestry is how the surface geometry influences reactivity. Single metal crystals with low Miller indices have often been used to probe the interactions between the reactive adsorbates and catalytic metal substrate. These low index surfaces are more accessible both computationally and experimentally, and have been essential to our current understanding of metal surface-catalyzed chemistry. However, the decreased complexity, because of the absence of active surface defects, can result in incomplete models of actual catalytic systems. Actual catalytic surfaces are believed to possess many defect sites that contribute to the overall reactivity of the catalyst. It has been recently shown that differences in the (110) and (100) step edge greatly influences water structures on the Pt surface. By using highly stepped Pt crystals with (110) and (100) steps, we see that the slight geometric differences between the (110) and (100) step also has profound effects on oxygen adsorption on stepped Pt crystals.

By utilizing highly stepped Pt crystals to study oxygen adsorption, along with ultra-high vacuum (UHV) surface science techniques such as temperature programmed desorption (TPD) and low temperature UHV scanning tunneling microscopy (STM), we are able to further understand O-Pt interactions on a surface that better mimics actual catalytic environments. Pt(553), with (110) step edges, was studied via STM to support the different behavior seen in oxygen adsorption between the (110) and (100) step edges in TPD experiments. The combination of TPD, STM, and variation in crystal step edge geometry allows for a more complete understanding of O_2 adsorption and dissociation on the Pt(553) surface and, more generally, (110) and (100) type step edges on Pt crystals.

9:00am **HC+SS-ThM4 Vibrational Symmetry Effects in the Dissociative Chemisorption of CH_2D_2 on Ni(111)**, *Arthur Utz*, *N. Chen*, *E.H. High*, Tufts University

Vibrational state resolved reactivity measurements have established that mode-selective chemistry, in which the reaction probability, S_0 , depends on the identity of the reactant's vibrational state, and bond selective chemistry, in which the product identity depends on the reagent's vibrational state, is widespread in the dissociation of methane and its isotopologues on Ni and Pt surfaces. Two factors lead to the observed mode- and bond-selectivity. First, methane's distorted transition state geometry introduces a bias that favors those vibrational motions that best access the transition state geometry. The sudden vector projection (SVP) model of Guo and coworkers predicts selectivity based on this factor. As the methane molecule approaches the surface, the molecule-surface interaction potential can also perturb the molecule's vibrations and lead to vibrational energy redistribution in the entrance channel for the reaction. Reaction path Hamiltonian calculations by Jackson and coworkers, quantum dynamics calculations by Kroes et al., and the vibrational adiabatic predictions of Halonen et al. focus on how this second factor impacts reactivity. In all of these calculations, the incident molecule's vibrational state symmetry can influence the vibrational coupling channels and energy flow pathways for the molecule as it approaches the surface.

This talk will focus on state-resolved experimental measurements of CH_2D_2 dissociation on a 90K Ni(111) surface. Unlike CH_4 , the C_{2v} symmetry of the CH_2D_2 molecule results in both the ν_1 symmetric- and ν_6 antisymmetric C-H stretching vibrations being infrared active. Therefore, we can use state-resolved infrared laser excitation of CH_2D_2 in a supersonic molecular beam to measure the reaction probability for these two C-H stretching states as a function of incident translational energy (E_{trans}). By performing the measurements at 90K, we observe a sharp energy threshold for reaction that permits an unusually precise measure of the efficacy of each vibration in promoting reaction. Our choice of excitation transitions further reduces experimental error in comparing the two states' reactivity. Contrary to the predictions of a vibrationally adiabatic model, the two states have nearly identical reaction probability. We will compare these results with recent reaction path Hamiltonian calculations from the Jackson group to explore how the symmetry of these two vibrational states impacts their reactivity.

Thursday Morning, November 10, 2016

9:20am **HC+SS-ThM5 Elementary Steps in Surface Reactions: Mechanisms, Kinetics and Thermodynamics**, *Swetlana Schauer mann*, Christian-Albrechts-Universität Kiel, Germany **INVITED**

Atomistic-level understanding of surface processes is a key prerequisite for rational design of new catalytic and functional materials. In our studies, we investigate mechanisms, kinetics and thermodynamics of heterogeneously catalyzed reactions and adsorption processes on nanostructured model supported catalysts by combination of multi-molecular beam techniques, infrared reflection-absorption spectroscopy and single crystal adsorption calorimetry. By employing these methods under well-defined ultra high vacuum conditions, we study mechanistic details of complex multi-pathway surface reactions, such as hydrocarbon transformation in presence of hydrogen or selective hydrogenation of multi-unsaturated hydrocarbons. The ultimate goal of our research is obtaining detailed correlations between reactivity, selectivity and the particular structure of the catalytic surface.

Specifically, it will be shown that selective hydrogenation of the C=O bond in acrolein to form an unsaturated alcohol is possible over Pd(111) with nearly 100 % selectivity. However, this process requires a very distinct modification of the Pd(111) surface with an overlayer of oxopropyl spectator species that are formed from acrolein during the initial stages of reaction and turn the metal surface selective towards propenol formation.

In the second part, a mechanistic picture of interaction of water with model $\text{Fe}_3\text{O}_4(111)/\text{Pt}(111)$ surface will be discussed. A combination of single crystal adsorption calorimetry and infrared spectroscopy was employed to determine the adsorption and dissociation heats of water and identify the surface species. We show that water dissociates readily on iron oxide surfaces forming a dimer-like hydroxyl-water complex and proved that the generally accepted model of water dissociation to two individual OH groups is incorrect.

11:00am **HC+SS-ThM10 CO_2 Hydrogenation on Rhodium: Comparative Study using Field Emission Techniques and 1-D Atom Probe**, *Sten Lambeets*, Université Libre de Bruxelles, Belgium; *C. Barroo*, Harvard University; *S. Owczarek*, *N. Gills*, Université Libre de Bruxelles, Belgium; *N. Kruse*, Washington State University; *T. Visart de Bocarmé*, Université Libre de Bruxelles, Belgium

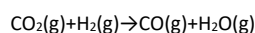
Valorization of CO_2 into useful products is one way to fulfill current environmental and economic imperatives. This can be done via the selective reduction of CO_2 using heterogeneous catalysts. To get a better understanding of the fundamental processes, we studied the CO_2 adsorption as well as its interaction with H_2 on single nanosized Rh crystals. For this, Field Emission Microscopy (FEM), Field Ion Microscopy (FIM) and 1-D Atom Probe (1DAP) were used. These methods use samples prepared as sharp needles, the extremity of which is imaged with nanoscale (FEM) and even with atomic lateral resolution (FIM).

The structure of the Rh nanocrystals is characterized by FIM, and CO_2 adsorption, dissociation and hydrogenation is studied in FEM mode. The brightness intensity of the FEM pattern depends on the presence and the nature of adsorbates. Probing and analyzing the brightness signal over time allows to qualitatively monitor the variations of surface composition, and thus the presence of surface reactions, during the ongoing processes.

Finally, 1DAP, which corresponds to the combination of a FIM device with mass spectrometry, is used to identify the nature of the different surface species.

The FEM pattern of a clean sample essentially highlights {012} facets. During CO_2 exposure, the brightness of these facets drastically decreases and remains dark, reflecting the CO_2 dissociative adsorption over these facets - leading to the formation of O(ad) species. The presence of O(ad) at the surface induces a new FEM pattern where {113} facets become the most visible. This pattern reflects the formation of subsurface oxygen O(sub) beneath the {113} facets, which is confirmed by comparison with N_2O , O_2 and CO on Rh systems. To study the hydrogenation of CO_2 , pure H_2 gas is introduced while the pressure of CO_2 is kept constant. Reaction phenomena, proved by variations in the brightness pattern, were observed from 650 to 734 K.

The adsorption of hydrogen at the surface leads to the formation of H(ad) species reacting with O(ad) to form $\text{H}_2\text{O(ad)}$. Similar reaction phenomena were also observed with $\text{N}_2\text{O}+\text{H}_2/\text{Rh}$ and $\text{O}_2+\text{H}_2/\text{Rh}$ systems in the same temperature range, but not with the $\text{CO}+\text{H}_2/\text{Rh}$ system, proving the role of O(ad) in the mechanism. Our observations allow to identify the reaction as the Reverse Water Gas Shift:



These assumptions are in line with direct local chemical first analyses performed by 1DAP. Rhodium oxides species - RhO^{2+} and RhO_2^{2+} - and CO_2 with its dissociation products, i.e. CO_2^+ , CO^+ and O^+ , are detected in the first layers of a (115) facet of the Rh nanoparticle during an exposure to pure CO_2 at 325 K.

11:20am **HC+SS-ThM11 State-resolved Reactivity of Methane on Ir(110)-(1x2)**, *Eric Peterson*, *E. Nicotera*, *E.K. Dombrowski*, *A.L. Utz*, Tufts University

The rate-limiting step in the steam reforming reaction, in which methane and water react to form hydrogen gas and carbon monoxide (syngas), is the initial cleavage of a C-H bond in the methane molecule. Methane's dissociative chemisorption is highly activated on catalytically active transition metal surfaces. To date, experimental measurements have focused on CH_4 molecules whose internal (vibrational) energy is less, and frequently much less than the threshold energy for reaction. Under those conditions, significant incident translational energy (TE) or energy transfer from the surface is required to activate dissociation, and reactions most often proceed via a direct dissociative chemisorption mechanism. Using a molecular beam in conjunction with an OPO-OPA continuous-wave IR laser, we are able to prepare methane molecules with a sharply defined kinetic energy and 36 kJ/mol of internal vibrational energy, which approaches or even exceeds the threshold energy for dissociative chemisorption. These molecules possess sufficient energy to react via direct or precursor-mediated mechanisms. The direct channel is characterized by an increase in reactivity with increasing TE, and is dominant for molecules with >10 kJ/mol of TE. Molecules with <10 kJ/mol of energy react through precursor-mediated channel, in which reactivity decreases with increasing TE. This low-TE precursor channel is especially interesting in a catalytic context, as most molecules under typical industrial reactor conditions have TEs where trapping, and therefore physisorption probabilities are high.

In studies of CH_4 dissociation on Ir single crystal surfaces, we observe both the precursor and direct channels for reaction. On Ir(111) we observe that 36 kJ/mol of E_{vib} in the n_3 C-H stretch enhances reactivity in both channels at a surface temperature of 1000K. On the corrugated Ir(110)-(1x2) surface, we still observe vibrational-energy enhancement in both channels, but the TE dependence of S_0 differs for the vibrationally hot and ground state CH_4 molecules at $T_{\text{surf}} = 1000\text{K}$. Upon lowering T_{surf} to 500K, vibrational ground state molecules no longer have a pronounced precursor-mediated reaction channel, but the vibrationally excited molecules do. We will discuss the origin of these similarities and differences. The observed reactivity of vibrationally hot methane molecules with thermal TE points to the potentially important role that vibrationally hot precursor molecules may play in industrially catalyzed reactors.

11:40am **HC+SS-ThM12 Curved Single Crystals As Tools to Study Structure Dependences in Surface Science and Gas-Surface Reactions Dynamics**, *Ludo Juurlink*, Leiden University, Netherlands **INVITED**

The surface science approach has benefited for many decades from the availability of flat single crystal samples of high purity and high surface quality. The traditional flat, polished samples provide the user with a single surface structure that dominates over macroscopic length scales. However, a single sample that provides the user with multiple surface structures may provide additional benefits. For example, in attempts to relate chemical reactivity or selectivity to surface structure, having a continuous range of vicinal surfaces in a single sample can speed up scientific research and circumvent experimental difficulties. Also for studies focusing on either short or long-range effects in adsorbates and electronic states that are perturbed by steps, a single sample with a range of surface structures is an excellent tool. Therefore, we have revived the implementation of curved single crystal surfaces in traditional surface science studies and elaborated the implementation toward gas-surface reaction dynamics. Depending on the bulk crystal structure and the directions of the apex and curvature, many different surface structures are available in a single sample. We show how we now use LEED, AES, STM, TPD, RAIRS and supersonic molecular beam techniques to directly relate surface structure to molecular and dissociative adsorption, desorption, and chemical reactions. We exemplify the possibilities by showing recent results from studies that used a cylindrical Ni single crystal, two curved Ag samples, a Co curved sample and two Pt curved single crystal surfaces with various apex directions.

Fundamental Discoveries in Heterogeneous Catalysis Focus Topic

Room 103A - Session HC+SS-ThA

Advances in Theoretical Models and Simulations of Heterogeneously-catalyzed Reactions

Moderator: Donna Chen, University of South Carolina

2:20pm **HC+SS-ThA1 Theoretical Pathways to Predict (meta-)stability of Gas Phase Metal Oxide Clusters: Beyond the Static Mono-Structure Description, *Saswata Bhattacharya***, Indian Institute of Technology Delhi, India; *L.M. Ghiringhelli*, Fritz-Haber-Institut der Max-Planck-Gesellschaft; *N. Marom*, Tulane University

This talk is driven by the vision of computational design of cluster-based nanocatalysts. The discovery of the extraordinary activity in catalysis exhibited by small metal-oxide clusters has stimulated considerable research interest. However, in heterogeneous catalysis, materials property changes under operational environment (e.g. temperature (T) and pressure (p) in an atmosphere of reactive molecules). Therefore, a solid theoretical understanding at a realistic (T, p) is essential in order to address the underlying phenomena. In this talk, I shall first introduce a robust methodological approach that integrates various levels of theories combined into one multi-scale simulation to address this problem[1]. I shall show one application of this methodology in addressing (T, p) dependence of the composition, structure, and stability of metal oxide clusters in a reactive atmosphere at thermodynamic equilibrium using a model system that is relevant for many practical applications: free metal (Mg) clusters in an oxygen atmosphere[2].

More recently, I have extended this development in designing clusters with desired properties. The novelty of this implementation is that it goes beyond the interpretation of experimental observations and addresses the challenging "inverse problem" of computationally designing clusters with target properties. The methodology is applied and thoroughly benchmarked on $(\text{TiO}_2)_n$ clusters [$n=2, 3, \dots, 10, 15, 20$][3]. All the results are duly validated using the highest level of theories currently achievable within Density Functional Theory (DFT).

References:

- [1] S. Bhattacharya, S. Levchenko, L. Ghiringhelli, M. Scheffler, *New J. Phys.* 16, 123016 (2014).
- [2] S. Bhattacharya, S. Levchenko, L. Ghiringhelli, M. Scheffler, *Phys. Rev. Lett.* 111, 135501 (2013).
- [3] S. Bhattacharya, B. Sonin, C. Jumonville, L. Ghiringhelli, N. Marom, *Phys. Rev. B* 91, 241115 (R), (2015).

2:40pm **HC+SS-ThA2 Role of Oxygen at the Surface and Subsurface during Catalytic Oxidation by Silver, *Sharani Roy***, University of Tennessee

Catalytic oxidation by the silver surface is used in several important industrial processes, such as epoxidation of ethylene to form polyethylene or partial oxidation of methane to form methanol. To understand the mechanisms of catalytic oxidation at the molecular level, it is essential to understand the interactions of atomic oxygen with the silver surface. We present a detailed theoretical study of oxygen adsorbed on the surface and subsurface of silver based on density functional theory and molecular dynamics simulations. Our ultimate goal is to develop a conceptual model of reactivity of surface oxygen and subsurface oxygen in catalytic oxidation by the silver surface. While the detailed quantum chemical calculations serve to accurately model the ground-state potential energy landscape of the oxygen-silver system, molecular dynamics simulates the motion of oxygen on the surface and subsurface at realistic laboratory or catalytic temperatures. We focus on several important phenomena, including surface-site preference, coverage dependence, and temperature dependence of oxygen adsorption at the surface and subsurface. We also investigate the changes in the surface structure of silver induced by the presence of oxygen. Due to the differences in structure, interatomic spacing, and binding sites of the (111) and (110) faces of the silver crystal, the adsorption properties of atomic oxygen vary for the two surfaces. Our study determines some fundamental differences in silver-oxygen interactions on the two surfaces, and provides qualitative insight on how the choice of surface can affect the participation of surface and subsurface oxygen in catalytic oxidation by silver. Future work will explore the interactions of surface oxygen and subsurface oxygen with reactant molecules such as methane or ethylene.

Thursday Afternoon, November 10, 2016

3:00pm **HC+SS-ThA3 Using Theory and Computation to Understand Plasma Enhanced Dry Reforming on Nickel Catalysts, *George Schatz***, Northwestern University

INVITED

Dry reforming is a process wherein CH_4 and CO_2 react to give synthesis gas and/or liquid fuels. Dry reforming is normally done under high temperature and pressure conditions, with a Ni catalyst, however it has recently been discovered that if a plasma is also present near the catalyst, then it is possible to get this reaction to go under modest conditions close to room temperature and atmospheric pressure. The role of the plasma in this process is poorly understood. In this talk I will describe several electronic structure studies that my group is doing which are designed to describe the processes involved in plasma enhanced dry reforming, including both the role of the plasma, and the gas-surface chemistry that occurs in the presence of plasma species. The plasma is known to fragment the reacting gases, especially CH_4 , so we will study the interaction of methane fragments with various Ni surfaces, to show how this enhances chemisorption, surface dissociation, and subsequent reaction with species already on the surface. A highlight of this work involves the reaction of subsurface hydrogen with adsorbed CO_2 to give CO, water and other products. We have also studied the influence and ions and electrons on surface chemistry.

4:00pm **HC+SS-ThA6 The Impact of Structure on the Catalytic Behavior of Cu_2O Supported Pt Atoms, *Andrew Therrien***, Tufts University Department of Chemistry; *E.C.H. Sykes*, Tufts University

Single site catalysts composed of individual atoms on various oxide supports have been a major research focus in recent years. Such catalysts exhibit novel reactivity with the benefit of 100% atom efficiency and a dramatic reduction in the precious metal loading. However, despite several experimental examples of efficient single atom catalysts, there is much debate regarding the structure and catalytic mechanisms of such catalysts and debate over whether single atoms or nanoparticles are the active species. Given the complexity of heterogeneous catalysts and the size scale of the active sites, there is a need for a surface science and microscopy approach to understand the structure and reactivity of atomically dispersed atoms on oxides.

We have studied the structure and reactivity of individual Pt atoms supported on oxidized Cu using scanning tunneling microscopy (STM) and temperature programmed reaction (TPR). We first elucidated the structure of the support, a previously observed but unsolved Cu_2O overlayer on Cu, by density functional theory (DFT) and comparison of simulated STM images with experimental STM. We discovered that the oxide surface is inert towards CO oxidation, while the single Pt atom decorated surface is efficient for low-temperature CO oxidation. This system is also capable of water activation. Our combination of TPR and STM studies suggest that single Pt atoms supported on the oxide are indeed catalytically active and may be a good catalyst for the water-gas shift reaction.

4:20pm **HC+SS-ThA7 Energetics of Water Dissociative Adsorption on $\text{NiO}(111)\text{-}2\times 2$, *Wei Zhao***, University of Washington; *M. Bajdich*, Stanford University; *S. Carey*, University of Washington; *M. Hoffmann*, A. Vojvodic, J. Nørskov, Stanford University; *C.T. Campbell*, University of Washington

The energetics of the reactions of water with metal oxide surfaces are of tremendous interest for catalysis and electrocatalysis, yet the energy for the dissociative adsorption of water was only previously known on one well-defined oxide surface, $\text{Fe}_3\text{O}_4(111)$. [1] Here we report the first calorimetric measurement of the heat of reaction for the dissociative adsorption of water on $\text{NiO}(111)\text{-}2\times 2$ as a function of coverage, showing that the heat of dissociative adsorption decreases with coverage from 177 kJ/mol to 119 kJ/mol in the first 0.25 ML of coverage. These measurements provide an important benchmark for validating computational estimates of adsorption energies of molecular fragments on correlated metal-oxide such as NiO and for oxide surface chemistry in general, which is more challenging in this respect than for metal or wide-gap semiconductor surfaces. We also present DFT calculations of the energetics of this reaction, and compare it to the calorimetric results.

- [1] P. Demontyev, K.-H. Dostert, F. Ivars-Barceló, C.P. O'Brien, F. Mirabella, S. Schauerhmann, X. Li, J. Paier, J. Sauer, H.-J. Freund, *Water Interaction with Iron Oxides*, *Angewandte Chemie International Edition*, 54 (2015) 13942-13946.

* Morton S. Traum Award Finalist

Thursday Afternoon, November 10, 2016

4:40pm HC+SS-ThA8 Challenges in the First-Principles Description of Reactions in Electrocatalysis, *Axel Groß*, Ulm University, Germany INVITED

In spite of its technological relevance in the energy conversion and storage, our knowledge about the microscopic structure of electrochemical electrode-electrolyte interfaces and electrical double layers is still rather limited. The theoretical description of these interfaces from first principles is hampered by three facts. i) In electrochemistry, structures and properties of the electrode-electrolyte interfaces are governed by the electrode potential which adds considerable complexity to the theoretical treatment since charged surfaces have to be considered. ii) The theoretical treatment of processes at solid-liquid interfaces includes a proper description of the liquid which requires to determine free energies instead of just total energies. This means that computationally expensive statistical averages have to be performed. iii) Electronic structure methods based on density functional theory (DFT) combine numerical efficiency with a satisfactory accuracy. However, there are severe shortcomings of the DFT description of liquids, in particular water, using current functionals.

Despite these obstacles, there has already significant progress been made in the first-principles modeling of electrochemical electrode-electrolyte interfaces. In this contribution, I will in particular focus on how the electrochemical environment can be appropriately taken into account using numerically efficient schemes. In the presence of an aqueous electrolyte, metal electrodes are in general covered by either cations or anions. Based on the concept of the computational hydrogen electrode, the equilibrium coverage of Pt(111) with hydrogen (1,2) and halides (3) as a function of the electrode potential has been derived showing that halide and hydrogen adsorption is competitive, in agreement with experimental findings. The presence of the aqueous electrolyte has been taken into account modeling water layers either implicitly through a polarizable medium (2) or explicitly in ab initio molecular dynamics runs (3). To obtain a proper description of the water-water and the water-metal interaction, it turns out that the consideration of dispersion corrections is essential (4). The importance of the electrochemical environment in electrocatalytic processes will be demonstrated using the methanol electrooxidation on Pt(111) (5) as an example.

References

- (1) S. Sakong, M. Naderian, K. Mathew, R. G. Hennig, and A. Gross, *J. Chem. Phys.* **142**, 234107 (2015).
- (2) T. Roman and A. Gross, *Catal. Today*. **202**, 183 (2013).
- (3) F. Gossenberger, T. Roman, and A. Gross, *Surf. Sci.* **631**, 17 (2015).
- (4) K. Konigold and A. Gross, *J. Comput. Chem.* **33**, 695(2012).
- (5) S. Sakong and A. Gross, submitted.

5:20pm HC+SS-ThA10 Beyond the 2D Lattice Gas and 2D Ideal Gas Models for Adsorbates: The Hindered Translator / Hindered Rotor Model, *Liney Arnadottir*, *L.H. Sprowl*, Oregon State University; *C.T. Campbell*, University of Washington

With the recent explosion in computational catalysis and related microkinetic modeling, the need for a fast yet accurate way to predict equilibrium and rate constants for surface reactions has become more important. In such calculations, adsorbates are usually treated within either the 2D lattice gas or 2D ideal gas approximation to estimate their partition functions and entropies. Here we present a fast new method to estimate the partition functions and entropies of adsorbates that is much more accurate than those approximations, and recognizes the true oscillating nature of the adsorbate's potential energy for motions parallel to the surface. As with previous approaches, it uses the harmonic oscillator (HO) approximation for most of the modes of motion of the adsorbate. However, it uses hindered translator and hindered rotor models for the three adsorbate modes associated with motions parallel to the surface, and evaluates these using an approach based on a method that has proven accurate in modeling the internal hindered rotations of gas molecules. The translational and rotational contributions to the entropy of a hindered translator / hindered rotor calculated with this new method are, in general, very closely approximated (to within $<0.25R$ error per mode) by the corresponding harmonic oscillator (i.e., 2D lattice gas) entropy when kT is less than the barrier. When kT exceeds the barrier, the hindered translator / hindered rotor model is closely approximated (to within $0.1 R$) by the entropy of an ideal 2D gas. The harmonic oscillator / lattice gas model severely overestimates the entropy when kT greatly exceeds the barrier. The cutoff between the temperature ranges of applicability of these simple two approximations is very sharp but with our combined hindered

rotor/hindered translator approach the whole temperature range is covered with the same approach.

5:40pm HC+SS-ThA11 Methanol Partial Oxidation Catalyzed by Singly-dispersed Pd on ZnO(101 $\bar{0}$), *Takat B. Rawal*, *S.R. Acharya*, *S. Hong*, *T.S. Rahman*, University of Central Florida

Heterogeneous catalysis by singly-dispersed metal atoms on non-metallic surfaces offers great potential for maximizing the efficiency of metal atoms, and optimizing their activity and selectivity. Herein, we present results from our *ab-initio* density functional theory (DFT) calculations for methanol partial oxidation (MPO), an industrially important reaction for the production of H_2 , on Pd $_1$ /ZnO(101 $\bar{0}$). To begin with we find that the Pd atom prefers to adsorb at the oxygen vacancy site i.e. the anion vacancy is responsible for stabilizing singly-dispersed Pd atom on ZnO(101 $\bar{0}$). We discuss the adsorption characteristics of a set of gas molecules (CH_3OH , O_2 , CO , CO_2 , H_2O , H_2), and the potential energy profile including activation barriers for the reaction processes associated with MPO on Pd $_1$ /ZnO(101 $\bar{0}$), and compare them with those on Pd $_{16}$ Zn $_{16}$ nanoparticle and pristine ZnO(101 $\bar{0}$). We find that the singly dispersed Pd sites offer a high activity towards the formation of CO_2 and H_2 over that of CO and H_2O . We trace this reactivity to the electronic structure of the single Pd site as modified by its local environment which in turn facilitates a strong binding of CO to the Pd site, thereby increasing the CO desorption barrier and stabilizing O_2 on ZnO(101 $\bar{0}$), which is essential for further oxidation steps. With activation energy barriers and pre-exponential factors calculated from DFT, for a large set of reaction intermediates, we perform kinetic Monte Carlo simulations to determine the turn over frequencies and rate limiting steps in the formation of CO_2 and H_2 on Pd $_1$ /ZnO(101 $\bar{0}$), under ambient conditions.

Work supported in part by DOE grant DE-FG02-07ER15842.

6:00pm HC+SS-ThA12 Simulations of Surface Induced Dissociation, Soft Landing, and Reactive Landing in Collisions of Protonated Peptide Ions with Organic Surfaces, *William Hase*, *S. Pratihar*, Texas Tech University

Chemical dynamics simulations have been performed to explore the atomistic dynamics of collisions of protonated peptide ions, peptide- H^+ , with organic surfaces. Overall, the results of the simulations are in quite good agreement with experiment. The simulations have investigated the energy transfer and fragmentation dynamics for peptide- H^+ surface-induced dissociation (SID), peptide- H^+ physisorption on the surface, soft landing (SL), and peptide- H^+ reaction with the surface, reactive landing (RL). The primary structure of biological ions is determined by SID, as well as information regarding the ions' fragmentation pathways and energetics. SID occurs by two mechanisms. One is a traditional mechanism in which peptide- H^+ is vibrationally excited by its collision with the surface and then dissociates in accord with the statistical, RRKM unimolecular rate theory after it rebounds off the surface. For the other mechanism, the ion *shatters* via a non-statistical mechanism as it collides with the surface. The simulations have also provided important dynamical insight regarding SL and RL of biological ions on surfaces. SL and RL have a broad range of important applications including preparation of protein and peptide microarrays. The simulations indicate that SL occurs via multiple mechanisms consisting of peptide- H^+ physisorption on and penetration in the surface. An important RL mechanism is intact deposition of peptide- H^+ on the surface.

Surface Science

Room 104E - Session SS+HC-FrM

Deposition and Analysis of Complex Interfaces

Moderators: Bruce D. Kay, Pacific Northwest National Laboratory, Daniel Killelea, Loyola University Chicago

8:20am **SS+HC-FrM1 A Quantitative, Experimentally Supported Model for Surface Energy (SE) as a Function of Surface Defect Density (DD): the SEDD Model - Comparison with Three Liquid Contact Angle Analysis and AFM, Abijith Krishnan**, Arizona State University/BASIS HS Scottsdale/SiO2 Innovates LLC; *N.X. Herbots*, Arizona State University/SiO2 Innovates LLC; *Y.W. Pershad*, Arizona State University/BASIS HS Scottsdale/SiO2 Innovates LLC; *S.D. Whaley*, SiO2 Innovates LLC/Arizona State University; *R.J. Culbertson*, *R.B. Bennett-Kennett*, Arizona State University

Metal Oxide Semiconductor Field Emission Transistors (MOSFETs) have been key to micro- and nano-electronics for the past six decades, but electrically active defects resulting from dangling bonds (unbounded electrons) or mobile ions create parasitic charges, known as surface charges (Q_{ss} for dangling bonds and Q_o for mobile ions), that limit performance. Passivation via oxygen and hydrogen species can reduce surface defects. However, surface state charge analysis via capacitance-voltage (C-V) curves is used to evaluate the extent of passivation but does not accurately reflect the number of structural defects. On the other hand, surface characterization by Tapping Mode Atomic Force Microscopy (TMAFM) can be used for topographic observation and surface roughness measurements but has not been used to measure surface defect density. The new theoretical model proposed the Surface Energy Defect Density (SEDD) Model [1] aims to relate surface defect density to surface energy, a macroscopic quantity measured via high statistics Three Liquid Contact Angle Analysis (3LCAA) metrology [2,3]. Three Liquid Contact Angle Analysis (3LCAA) conducted in a class 100 clean-room using the Sessile Drop method and the Van Oss theory enables for accurate and reproducible contacts angles analysis within 1°, and a reproducible relative error lower than 2-3% for the total surface energy. These results have led to the conception a new theoretical model, the Surface Energy -Defect Density Model (SEDD) which relates the macroscopic surface energy density to the microscopic defect density. To test this model with experimental defect densities, this work uses PIXNANOVERT, a new algorithm to extract defect densities from high resolution large area (1 x10 μm^2) TMAFM topographs taken on Si(100) passivated by the Herbots-Atluri process [5-7]. Analysis using surface effect density extracted. PIXNANOVERT shows that the SEDD Model predicts, within 5 the measured surface defect densities of oxidized Si surfaces with known surface energies. With this model, MOSFET manufacturers can determine the defect density in the oxide interface of their transistors by measuring the surface energy of the oxide. Testing transistor effectiveness for computers and other electronic devices would thus become more accurate than relying on C-V curves to quantify surface charge density. The SEDD Model would also allow us to determine the surface chemistry (e.g. hydrophobicity) of many other crystalline or amorphous materials, such as polymers and glasses, by measuring the surface energy.

[1] AS Krishnan, Senior Thesis (2016)

[2] Pat. pend., Herbots et al. (2011,2012,2016)

[3] SD Whaley, PhD, ASU (2013)

8:40am **SS+HC-FrM2 Ab initio Analysis of Elementary Reactions during ALD Tungsten Nucleation on Selective Substrates, Mariah King, G.N. Parsons**, North Carolina State University

In 1987, selective deposition of tungsten via silane reduction was confirmed with a high deposition rate at a low temperature. Despite the numerous studies that have been conducted in the following years, many chemical processes that control selective tungsten ALD growth are not yet sufficiently understood and the leading concern remains that, past the "selective window", uniform deposition is observed on silica, the non-reactive surface. This loss of selectivity is due to the ability of the non-selective surface to promote nucleation in time due to surface processes and chemical reactions. The primary cause of tungsten nucleation on silica is a long-standing problem in the semiconductor industry that will require new fundamental understanding and an accurate description of the reaction kinetics between reactants and substrates at the atomic level.

In this computational study, we use density functional theory to study the reaction energetics, structural stability, and electronic distribution to describe initial reactions during ALD tungsten nucleation on silicon, silica and tungsten substrates. The objective is to identify reactions that have a lower probability of occurrence, but may lead to defects that enable nucleation on otherwise non-reactive surfaces. Understanding the probability at which a species reacts with a pristine non-reactive surface will enable designers to define the limits of process defect generation, thereby identifying viable process options. Additionally, these simulations are used to suggest alternative system conditions that could lead to improved selectivity.

As a first step towards understanding the kinetics of complex deposition reactions, we present the kinetics of the elementary reactions for silane and tungsten deposition on silica and fluorinated tungsten surfaces. Along with intensive experimental data on this specific system, we have used the calculated reaction energetics to suggest the most probable series of reactions that lead to loss of selectivity. Extending these results will allow us to define viable options and directions for highly selective processes that minimize defect creation and propagation in electronic device manufacturing.

9:00am **SS+HC-FrM3 Design and Synthesis of Nanofence Cerium Oxide Coated Platinum Catalysts via Facet-selective Atomic Layer Deposition, Kun Cao, J.M. Cai**, State Key Laboratory of Digital Manufacturing Equipment and Technology, Huazhong University of Science and Technology, China; *R. Chen*, State Key Laboratory of Digital Manufacturing Equipment and Technology, School of Mechanical Science and Engineering, School of Optical and Electronic Information, Huazhong University of Science and Technology, China

Sintering of Pt nanoparticles (NPs) catalysts at elevated working temperature is highly undesirable, as coalescence of NPs will cause significant decrease in the number of active sites and resulting catalytic performance degradation. Oxide overcoating techniques have been recently developed to minimize Pt sintering. However, certain trade-off has to be made between stabilization and reactivity. Stabilize metal nanoparticles and simultaneously enhance catalytic activity is still very challenging.

Here, we designed a cerium oxide nanofence coating structure to stabilize Pt NPs using facet selective atomic layer deposition. The facet selectivity is realized through differences in binding energy of Ce precursor fragments Pt surfaces. CeO_x prefers to selectively deposit on Pt (111) facets, while leaving the Pt (100) surface intact. CeO_x has synergy with metal as coating layer and creates highly active sites at Pt-CeO_x interfaces. From stability point of view, CeO_x anchors Pt NPs with a strong metal oxide interaction, and nanofence coating layer provide physical blocking that suppresses NP particle migration. Such nanofence CeO_x coated Pt catalysts show both enhanced CO conversion activity and improved sintering resistance up to 700 °C under oxidative atmospheric condition.

9:20am **SS+HC-FrM4 Dehydrogenation and Rehybridization of ZnTPP on Ag(100) and Ag(111), C. Ruggieri, S. Rangan, Robert Bartynski**, Rutgers, the State University of New Jersey; *E. Galoppini*, Rutgers - Newark

The interactions between zinc(II) tetraphenylporphyrin (ZnTPP) molecules and the Ag(100) and Ag(111) surfaces were investigated using a combination of scanning tunneling microscopy as a local probe of the molecular adsorption configuration and X-ray, ultraviolet, and inverse photoemission spectroscopies as probes of the electronic structure. When forming a molecular monolayer by desorption of a multilayer on the Ag(100) surface, an order molecular array in registry with the substrate and having a square unit cell results. A similar preparation on the Ag(111) surface produces an overlayer that is considerably less dense but is also commensurate with the substrate having a unit cell that is slightly rectangular. Subsequent annealing leads to a transition from intact molecular adsorption to dehydrogenation and subsequent intramolecular and intermolecular rehybridization. Upon annealing, the molecule flattens as the phenyl portions of the molecule form bonds with a neighboring pyrrole group. This leads to a measurable alteration of the electronic structure. In addition, we find evidence of bonding between neighboring rehybridized molecules, consistent with the formation of biphenylene-type structures, leading to the growth of extended two-dimensional covalently bound structures. Understanding basic rules for molecule-molecule hybridization, potentially templated by prior self-assembly, could enable the directed formation of large, complex, and ordered 2-dimensional arrays of organic or metalorganic units.

C. Ruggieri, S. Rangan, R.A. Bartynski, and E. Galoppini, J. Phys. Chem. C 120, 7575 (2016)

9:40am **SS+HC-FrM5 A Case Study of the SMSI Effects: CO Oxidation on the $\text{TiO}_x/\text{Pt}(111)$ Model Surfaces**, *Mingshu Chen, H. Li, X.F. Weng, H. Zhang, H.L. Wan*, Xiamen University, China

Well-ordered ultrathin TiO_x films were grown on $\text{Pt}(111)$ as model surfaces to probe the effects of the strong metal-support interaction (SMSI) on the catalytic performance. The model surfaces of $\text{TiO}_x/\text{Pt}(111)$ were prepared under UHV and characterized by low-energy electron diffraction (LEED) and Auger electron spectroscopy (AES). CO oxidation was tested for the model surfaces in a batch reaction cell as a function of the TiO_x coverages and structures. And a home-built reflection adsorption infrared spectroscopy (IRAS) was used for *in-situ* studying the surface species and stability of the model surfaces under the reaction conditions. The results show that catalytic activity could be improved significantly on the monolayer z-TiO_x , while a maximum is achieved at $0.3\sim 0.5$ ML for the w-TiO_x . The TiO_x thin films were found to be stable under CO oxidation conditions. The activation energy for CO oxidation reaction on the 1 ML $\text{z-TiO}_x/\text{Pt}(111)$ was found to be 46 kJ/mol, which is much lower than that of 87 kJ/mol on the clean $\text{Pt}(111)$ surface.

10:00am **SS+HC-FrM6 Toluene and Benzyl Radical Formation during Deoxygenation of Phenylmethanol on Rutile $\text{TiO}_2(110)$** , *Long Chen, R.S. Smith, B.D. Kay, Z. Dohnalek*, Pacific Northwest National Laboratory

Understanding the reaction pathways of lignin-derived molecules on catalyst surfaces is of great importance for the sustainable production of energy carriers. In this regard, the role of radicals in the reaction mechanisms leading to functionalized aromatics has been extensively argued. The involvement of radical species has been firmly established for a number of simpler reactions on high surface area oxide catalysts, such as oxidative coupling of methane and selective oxidation of propylene. However, the formation of free radicals is rarely demonstrated. In this work, the reaction pathways of simple lignin-derived aromatic alcohols, i.e. phenol, phenylmethanol, and 2-phenylethanol, on a prototypical model oxide surface, rutile $\text{TiO}_2(110)$, are studied using a combination of molecular beam dosing and temperature programmed desorption (TPD). For phenylmethanol, the coverage dependent TPD data show that about 40% of molecules adsorbed on the surface at a saturation coverage are converted to reaction products indicating that the reactions proceed on regular five-fold coordinated Ti sites. This is in contrast to aliphatic alcohols where the reactions are shown to proceed exclusively on bridging oxygen vacancy defect sites. The studies of OD-labelled phenylmethanol demonstrate that a fraction of OD hydrogen is transferred to the benzyl group to form toluene that desorbs between 300 K and 480 K. In the competing reaction, the OD hydrogen is converted to water at ~ 350 K. Once the OD hydrogen is depleted above 480 K, the remaining phenylmethoxy surface species dissociate yielding benzyl radicals in the gas phase. Combined, these results show that the conversion of phenylmethanol on $\text{TiO}_2(110)$ proceeds via a unique chemistry. In contrast, both phenol and 2-phenylethanol exhibit expected surface chemistry analogous to that of aliphatic alcohols. These findings reveal for the first time the formation of free radical species from the interaction of phenylmethanol with $\text{TiO}_2(110)$ and demonstrate a new direct mechanism for deoxygenation of lignin-derived benzylic alcohols to aromatics on TiO_2 .

Bold page numbers indicate presenter

— A —

Acharya, S.R.: HC+SS-ThA11, 19
 Ahmadi, M.: HC+NS+SS-WeA10, **14**
 Ahmed, W.: SS2+AS+HC+NS-TuM11, **8**
 Alducin, M.: SS1+AS+HC+NS-TuM5, 5
 Andahazy, W.: HC+NS+SS-WeA9, 13
 Anderson, S.: SS2+AS+HC+NS-TuM1, **7**
 Arbiol, J.: SS2+AS+HC+NS-TuM12, 8
 Arnadottir, L.: HC+SS-ThA10, **19**;
 SS1+AS+HC+NS-TuM11, 6
 Arrigo, R.: IS+HC-WeA1, 14; IS+HC-WeA9, **15**
 Auerbach, D.J.: SS1+AS+HC+NS-TuM5, 5

— B —

Baber, A.E.: HC+NS+SS-WeA9, **13**
 Babore, A.: SS+AS+HC-MoA9, **4**
 Badan, C.: HC+SS-ThM3, 16
 Baddorf, A.P.: HC+NS+SS-WeA4, 13
 Bajdich, M.: HC+SS-ThA7, 18
 Barroo, C.: HC+SS-ThM10, 17
 Bartynski, R.A.: SS+HC-FrM4, **20**
 Behafarid, F.: HC+NS+SS-WeA10, 14
 Bennett-Kennett, R.B.: SS+HC-FrM1, 20
 Bhattacharya, S.: HC+SS-ThA1, **18**
 Blanco-Rey, M.: SS1+AS+HC+NS-TuM5, 5
 Bliem, R.: SS+AS+HC-MoA8, 4
 Bluhm, H.: SS+AS+HC-MoA10, 4; SS+AS+HC-MoM10, 2
 Boschen, J.S.: SS1+AS+HC+NS-TuM12, 6
 Boyle, D.T.: HC+NS+SS-WeA9, 13
 Brandt, A.J.: HC+SS-WeM6, 11
 Brown, R.D.: HC+SS-WeM5, **11**
 Bünermann, O.: SS1+AS+HC+NS-TuM5, 5

— C —

Cai, J.M.: SS+HC-FrM3, 20
 Camillone, N.: SS+AS+HC-MoA6, 3;
 SS1+AS+HC+NS-TuM2, 5
 Camillone, N.R.: SS+AS+HC-MoA6, 3;
 SS1+AS+HC+NS-TuM2, 5
 Campbell, C.T.: HC+SS-ThA10, 19; HC+SS-ThA7, 18; SS+AS+HC-MoA2, 3;
 SS1+AS+HC+NS-TuM11, 6; SS2+AS+HC+NS-TuM4, **7**
 Cao, K.: SS+HC-FrM3, **20**
 Carey, S.: HC+SS-ThA7, 18
 Carter, R.E.: SS+AS+HC-MoM8, 2
 Casey, S.M.: SS1+AS+HC+NS-TuM3, **5**
 Chen, D.A.: HC+SS-WeM6, **11**
 Chen, L.: SS+AS+HC-MoM2, 1; SS+HC-FrM6, **21**

Chen, M.S.: SS+HC-FrM5, **21**

Chen, N.: HC+SS-ThM4, 16

Chen, R.: SS+HC-FrM3, 20

Choi, H.: SS1+AS+HC+NS-TuM1, 5

Cohen, J.: SS2+AS+HC+NS-TuM5, **7**

Cohn, A.P.: SS+AS+HC-MoM8, 2

Culbertson, R.J.: SS+HC-FrM1, 20

Cutshall, D.B.: SS1+AS+HC+NS-TuM4, 5

— D —

Dahal, A.: SS+AS+HC-MoA1, **3**
 de la Mata, M.: SS2+AS+HC+NS-TuM12, 8
 de los Arcos, T.: SS+AS+HC-MoA11, 4
 DeBenedetti, W.J.I.: SS+HC-TuA2, 9
 Deng, X.: SS+AS+HC-MoM6, **1**
 Derouin, J.: HC+SS-WeM13, 12
 Diebold, U.: SS+AS+HC-MoA8, 4
 Dohnalek, Z.: HC+NS+SS-WeA1, **13**; SS+HC-FrM6, 21
 Dohnálek, Z.: SS+AS+HC-MoA1, 3; SS+AS+HC-MoM9, 2
 Dombrowski, E.K.: HC+SS-ThM11, 17
 Dorenkamp, Y.: SS1+AS+HC+NS-TuM5, 5
 Duke, A.S.: HC+SS-WeM6, 11
 — E —
 Einstein, T.L.: SS1+AS+HC+NS-TuM10, **6**

Eisenbraun, E.T.: SS2+AS+HC+NS-TuM3, 7

El Soda, M.: HC+NS+SS-WeA3, 13

Eren, B.: IS+HC-WeA3, **14**

Esan, D.A.: HC+SS-ThM1, **16**

Evans, J.W.: SS1+AS+HC+NS-TuM12, 6

— F —

Farber, R.G.: HC+SS-ThM3, **16**; HC+SS-WeM13, 12

Feeley, G.M.: SS2+AS+HC+NS-TuM4, 7

Field, D.A.: SS1+AS+HC+NS-TuM4, 5

Filler, M.A.: SS2+AS+HC+NS-TuM12, **8**

Franchini, C.: SS+AS+HC-MoA8, 4

— G —

Galoppini, E.: SS+HC-FrM4, 20

Geohagan, D.B.: SS+AS+HC-MoM8, 2

Ghiringhelli, L.M.: HC+SS-ThA1, 18

Gilis, N.: HC+SS-ThM10, 17

González, D.L.: SS1+AS+HC+NS-TuM10, 6

Groß, A.: HC+SS-ThA8, **19**

Grundmeier, G.: SS+AS+HC-MoA11, 4

— H —

Hansen, R.P.: SS2+AS+HC+NS-TuM3, **7**

Harrell, W.R.: SS1+AS+HC+NS-TuM4, 5

Harrison, I.: SS+HC-TuA8, 9

Harriss, J.E.: SS1+AS+HC+NS-TuM4, 5

Hase, W.L.: HC+SS-ThA12, **19**

Hävecker, M.: IS+HC-WeA1, 14

Head, A.R.: SS+AS+HC-MoA10, **4**

Heine, C.: IS+HC-WeA3, **14**

Hemminger, J.C.: SS+AS+HC-MoA9, 4

Hemmingson, S.L.: SS2+AS+HC+NS-TuM4, 7

Henderson, M.A.: SS+HC-TuA7, 9

Herbots, N.X.: SS+HC-FrM1, 20

Heyrich, H.: HC+SS-ThM3, 16

High, E.H.: HC+SS-ThM4, 16

Hines, M.A.: SS+HC-TuA2, 9

Hoffmann, M.: HC+SS-ThA7, 18

Hong, S.: HC+SS-ThA11, 19; SS1+AS+HC+NS-TuM13, 6

Hong, S.-Y.: SS+AS+HC-MoA6, 3;
 SS1+AS+HC+NS-TuM2, **5**

Hooper, D.: SS+AS+HC-MoM8, 2

Hui, H.: SS2+AS+HC+NS-TuM12, 8

Hulva, J.: SS+AS+HC-MoA8, **4**

— I —

Iski, E.V.: HC+SS-WeM12, **12**; HC+SS-WeM13, 12

— J —

Jackson, L.: HC+SS-WeM12, 12

Janke, S.M.: SS1+AS+HC+NS-TuM5, 5

Jiang, H.: SS1+AS+HC+NS-TuM5, 5

Jones, G.: HC+SS-WeM12, 12

Jones, T.E.: IS+HC-WeA1, 14

Juurlink, L.B.F.: HC+SS-ThM12, **17**; HC+SS-ThM3, 16

— K —

Kaden, W.E.: SS+HC-TuA12, **10**

Kaliakin, D.S.: SS1+AS+HC+NS-TuM3, 5

Kammler, M.: SS1+AS+HC+NS-TuM5, 5

Kandel, S.A.: HC+SS-WeM5, 11

Kandratsenka, A.: SS1+AS+HC+NS-TuM5, 5

Karslioglu, O.: SS+AS+HC-MoA10, 4;
 SS+AS+HC-MoM10, **2**

Kay, B.D.: SS+HC-FrM6, 21

Killelea, D.R.: HC+SS-ThM3, 16; HC+SS-WeM13, **12**

Kim, S.: SS+HC-TuA11, 10

Kim, Y.: HC+NS+SS-WeA7, 13

Kimmel, G.A.: SS+HC-TuA7, **9**

King, M.: SS+HC-FrM2, **20**

Knop-Gericke, A.: IS+HC-WeA1, **14**

Koel, B.E.: SS+HC-TuA1, **9**

Kondo, T.: HC+SS-ThM2, 16

Kozarashi, T.: HC+SS-ThM2, 16

Krishnan, A.S.: SS+HC-FrM1, **20**

Kroes, G.-J.: SS1+AS+HC+NS-TuM5, 5

Kronawitter, C.X.: SS+HC-TuA1, 9

Krooswyk, J.D.: HC+SS-WeM2, 11

Kruppe, C.M.: HC+SS-WeM2, **11**

Kruse, N.: HC+SS-ThM10, 17

Kuklja, M.M.: SS+AS+HC-MoA10, 4

Kulkarni, D.D.: SS1+AS+HC+NS-TuM4, **5**

— L —

Lam, V.: HC+NS+SS-WeA9, 13

Lambeets, S.V.: HC+SS-ThM10, **17**

Lee, C.: SS1+AS+HC+NS-TuM1, 5

Lee, H.: SS1+AS+HC+NS-TuM1, **5**

Lee, J.: SS+AS+HC-MoM6, 1; SS1+AS+HC+NS-TuM12, 6

Lee, Y.K.: SS1+AS+HC+NS-TuM1, 5

Li, H.: SS+HC-FrM5, 21

Lian, T.: SS+HC-TuA3, **9**

Liu, D.-J.: HC+NS+SS-WeA7, 13;
 SS1+AS+HC+NS-TuM12, **6**

Liu, S.: SS+AS+HC-MoA6, 3

Lownsbury, J.: SS+AS+HC-MoA2, 3

Lucci, F.R.: HC+NS+SS-WeA3, 13

Lundgren, E.: HC+SS-WeM3, **11**

Lyubnitsky, I.: SS+AS+HC-MoA1, 3

— M —

Ma, S.: SS+HC-TuA8, **9**

Maaß, S.: SS+AS+HC-MoA8, 4

Maddumapatabandi, T.D.: HC+SS-WeM6, 11

Maksymovych, P.: HC+NS+SS-WeA4, 13

Mallouk, T.E.: SS+AS+HC-MoA2, 3

Marcinkowski, M.D.: HC+NS+SS-WeA3, **13**

Marom, N.: HC+SS-ThA1, 18

Maruyama, B.: SS+AS+HC-MoM8, 2

McCann, J.P.: SS+AS+HC-MoM2, 1

McClimon, J.B.: SS2+AS+HC+NS-TuM10, 7

McEntee, M.: HC+NS+SS-WeA4, 13

Meier, M.: SS+AS+HC-MoA8, 4

Monazami, E.: SS2+AS+HC+NS-TuM10, **7**

Morales-Cifuentes, J.R.: SS1+AS+HC+NS-TuM10, 6

Morgan, H.: HC+SS-WeM12, 12

Mu, R.: SS+AS+HC-MoA1, 3

Mullins, D.R.: IS+HC-WeA4, **15**

— N —

Nakamura, J.: HC+SS-ThM2, **16**

Nakayama, K.S.: SS2+AS+HC+NS-TuM13, **8**

Nedrygaiov, I.: SS1+AS+HC+NS-TuM1, 5

Netzer, F.P.: HC+NS+SS-WeA1, 13;
 SS+AS+HC-MoM9, 2

Neurock, M.: HC+NS+SS-WeA4, 13

Nicotera, E.: HC+SS-ThM11, 17

Nikolaev, P.: SS+AS+HC-MoM8, 2

Nørskov, J.: HC+SS-ThA7, 18

Novotny, Z.: HC+NS+SS-WeA1, 13;
 SS+AS+HC-MoM9, 2

— O —

Oakes, L.: SS+AS+HC-MoM8, 2

Ogawa, T.: HC+SS-ThM2, 16

Oh, J.: HC+NS+SS-WeA7, 13

Ortoll-Bloch, A.: SS+HC-TuA2, 9

Overbury, S.H.: IS+HC-WeA4, 15

Owczarek, S.: HC+SS-ThM10, 17

— P —

Park, J.Y.: SS1+AS+HC+NS-TuM1, 5

Park, K.T.: SS+HC-TuA9, 9

Parkinson, G.S.: SS+AS+HC-MoA3, **3**;
 SS+AS+HC-MoA8, 4

Parsons, G.N.: SS+HC-FrM2, 20

Pavelec, J.: SS+AS+HC-MoA8, 4

Pavenelo, M.: SS1+AS+HC+NS-TuM5, 5

Pershad, Y.W.: SS+HC-FrM1, 20

Peterson, E.: HC+SS-ThM11, **17**

Peterson, E.W.: SS+AS+HC-MoA5, 3

Author Index

- Petrik, N.G.: SS+HC-TuA7, **9**
Pfeifer, V.: IS+HC-WeA1, **14**
Phillips, A.: HC+SS-WeM12, **12**
Phillips, R.S.: SS2+AS+HC+NS-TuM3, **7**
Pimpinelli, A.: SS1+AS+HC+NS-TuM10, **6**
Pint, C.L.: SS+AS+HC-MoM8, **2**
Pohlman, A.J.: SS1+AS+HC+NS-TuM3, **5**
Pratihari, S.: HC+SS-ThA12, **19**
Puzetzy, A.A.: SS+AS+HC-MoM8, **2**
— **Q** —
Quan, J.: HC+SS-ThM2, **16**
— **R** —
Rahman, T.S.: HC+SS-ThA11, **19**;
SS1+AS+HC+NS-TuM13, **6**
Rangan, S.: SS+HC-FrM4, **20**
Rao, R.: SS+AS+HC-MoM8, **2**
Rawal, T.B.: HC+SS-ThA11, **19**
Reinke, P.: SS2+AS+HC+NS-TuM10, **7**
Reish, M.: SS+HC-TuA8, **9**
Ren, Y.D.: HC+SS-ThM1, **16**
Robey, S.W.: SS+HC-TuA10, **9**
Rodriguez, J.: HC+SS-WeM10, **11**
Roldan Cuenya, B.: HC+NS+SS-WeA10, **14**;
IS+HC-WeA11, **15**
Rondinelli, J.M.: SS2+AS+HC+NS-TuM10, **7**
Roy, S.: HC+SS-ThA2, **18**
Ruggieri, C.: SS+HC-FrM4, **20**
— **S** —
Salmeron, M.B.: IS+HC-WeA3, **14**
Schatz, G.: HC+SS-ThA3, **18**
Schauermann, S.: HC+SS-ThM5, **17**
Schlögl, R.: IS+HC-WeA1, **14**
Schlosser, D.: HC+NS+SS-WeA9, **13**
Schmid, M.: SS+AS+HC-MoA8, **4**
Scott, S.L.: SS+AS+HC-MoM3, **1**
Share, K.: SS+AS+HC-MoM8, **2**
Shen, M.: SS+HC-TuA7, **9**
Sivaram, S.V.: SS2+AS+HC+NS-TuM12, **8**
Skibinski, E.S.: SS+HC-TuA2, **9**
Smith, R.S.: SS+HC-FrM6, **21**
Somaratne, D.: SS+HC-TuA11, **10**
Somorjai, G.A.: IS+HC-WeA3, **14**
Song, A.: SS+HC-TuA2, **9**
Sorescu, D.C.: SS+AS+HC-MoM6, **1**
Sosolik, C.E.: SS1+AS+HC+NS-TuM4, **5**
Sprowl, L.H.: HC+SS-ThA10, **19**;
SS1+AS+HC+NS-TuM11, **6**
Stotz, E.: IS+HC-WeA1, **14**
Sykes, E.C.H.: HC+NS+SS-WeA11, **14**;
HC+NS+SS-WeA3, **13**; HC+SS-ThA6, **18**
— **T** —
Tait, S.L.: SS+AS+HC-MoM1, **1**; SS+AS+HC-
MoM2, **1**
Tang, W.: HC+NS+SS-WeA4, **13**
Teplyakov, A.V.: SS2+AS+HC+NS-TuM6, **7**
Therrien, A.J.: HC+SS-ThA6, **18**
Thiel, P.A.: HC+NS+SS-WeA7, **13**;
SS1+AS+HC+NS-TuM12, **6**
Thuening, T.D.: HC+SS-WeM1, **11**
Tobin, R.G.: SS2+AS+HC+NS-TuM5, **7**
Tosti, N.: HC+NS+SS-WeA9, **13**
Trenary, M.: HC+SS-ThM1, **16**; HC+SS-WeM2,
11
Trotochaud, L.: SS+AS+HC-MoA10, **4**;
SS+AS+HC-MoM10, **2**
Tsyshevsky, R.: SS+AS+HC-MoA10, **4**
Turano, M.E.: HC+SS-WeM13, **12**
— **U** —
Uppuluri, R.: SS+AS+HC-MoA2, **3**
Utz, A.L.: HC+SS-ThM11, **17**; HC+SS-ThM4,
16
— **V** —
van Ruitenbeek, J.M.: SS2+AS+HC+NS-
TuM11, **8**
Varganov, S.A.: SS1+AS+HC+NS-TuM3, **5**
Velasco-Velez, J.J.: IS+HC-WeA1, **14**
Ventrice, Jr., C.A.: SS2+AS+HC+NS-TuM3, **7**
Visart de Bocarmé, T.: HC+SS-ThM10, **17**
Vojvodic, A.: HC+SS-ThA7, **18**
— **W** —
Walen, H.: HC+NS+SS-WeA7, **13**
Waluyo, I.B.: HC+SS-ThM1, **16**
Wan, H.L.: SS+HC-FrM5, **21**
Wang, J.: HC+NS+SS-WeA4, **13**
Wang, M.: SS+AS+HC-MoM1, **1**
Ward, T.Z.: IS+HC-WeA4, **15**
Weng, X.F.: SS+HC-FrM5, **21**
Whaley, S.D.: SS+HC-FrM1, **20**
White, M.G.: SS+AS+HC-MoA6, **3**;
SS1+AS+HC+NS-TuM2, **5**
Whitten, J.E.: SS+HC-TuA11, **10**
Wiesing, M.: SS+AS+HC-MoA11, **4**
Wilke, J.: HC+NS+SS-WeA9, **13**
Williams, C.: SS+AS+HC-MoM1, **1**
Williams, M.G.: SS2+AS+HC+NS-TuM6, **7**
Windus, T.L.: SS1+AS+HC+NS-TuM12, **6**
— **X** —
Xia, Y.: SS+HC-TuA9, **9**
Xie, K.: HC+SS-WeM6, **11**
Xu, P.: SS+AS+HC-MoA6, **3**; SS1+AS+HC+NS-
TuM2, **5**
— **Y** —
Yang, H.J.: HC+NS+SS-WeA7, **13**
Yates, Jr., J.T.: HC+NS+SS-WeA4, **13**; SS+HC-
TuA8, **9**
Yoshinobu, J.: SS+AS+HC-MoM5, **1**
— **Z** —
Zegkinoglou, I.: SS+AS+HC-MoM10, **2**
Zhang, H.: SS+HC-FrM5, **21**
Zhang, W.: SS+AS+HC-MoA2, **3**
Zhang, Z.: SS+HC-TuA8, **9**; SS+HC-TuA9, **9**
Zhao, W.: HC+SS-ThA7, **18**
Zhou, J.: SS+AS+HC-MoA5, **3**
Zhu, K.: SS+HC-TuA9, **9**